The Abdus Salam
International Centre for Theoretical Physics

United Nations
Educational, Scientific
and Cultural Organization

International Atomic
Energy Agency

SMR.1744 - 6

SCHOOL ON ION BEAM ANALYSIS AND ACCELERATOR APPLICATIONS

13 - 24 March 2006

Nuclear Reaction Analysis - Concept and application

Gabor BATTISTIG
Research Institute for Technical Physics and Materials Science
Budapest, Hungary

Strada Costiera 11, 34014 Trieste, Italy - Tel. +39 040 2240 111; Fax +39 040 224 163 - sci_info@ictp.it, www.ictp.it

Nuclear Reaction Analysis Resonances

Gábor Battistig

Research Institute for Technical Physics
and
Materials Science
(MTA - MFA)
Budapest, Hungary

battisti@mfa.kfki.hu

Inelastic nuclear collision with nuclear excitation

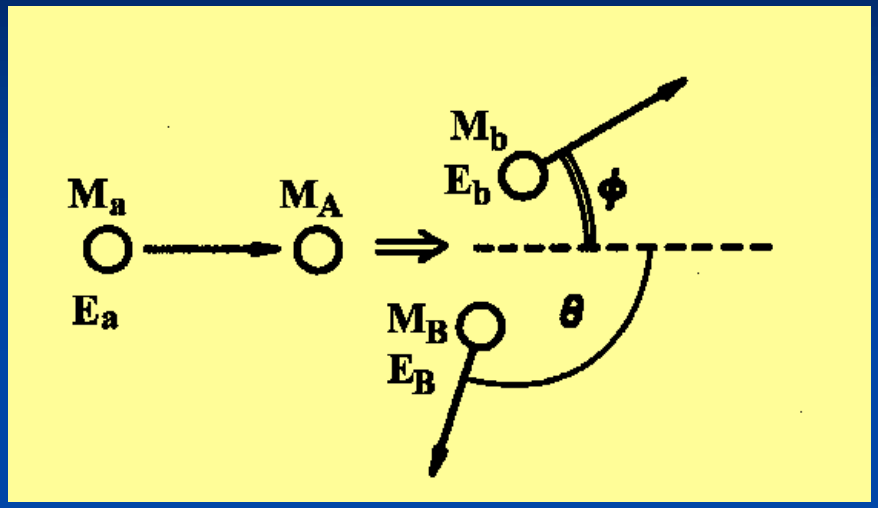

Nuclear reaction in general

$$A(a,b)B$$

Isotope specific!

Projectile energy must be higher than Coulomb barrier

$$A_A + A_a = A_b + A_B$$

$$Z_A + Z_a = Z_b + Z_B$$

$$E_a + E_A = E_b + E_B + Q$$

$$Q = (M_a + M_A - M_b - M_B)c^2$$

$$Q > 0 \rightarrow Exoterm$$

$$Q < 0 \rightarrow Endoterm$$

$$E_c = \frac{Z_A Z_a e^2}{R} \approx Z_A Z_a A_A^{-\frac{1}{3}} [MeV]$$

$$E_{th} = -Q \frac{M_B + M_b}{M_B + M_b - M_a}$$

Ion-Gamma reaction : $^{19}F(p,\gamma)^{20}Ne$ Q=12.845 MeV

Ion-Ion reaction : $^{19}F(p,\alpha)^{16}O$ Q=8.115 MeV

Ion-Neutron reaction : $^{19}F(p,n)^{19}Ne$ Q=-4.020 MeV

Particle Induced Activation Analysis (PAA) : $^{19}F(p,n)^{19}Ne$ $\beta^+ \rightarrow$ ^{19}F

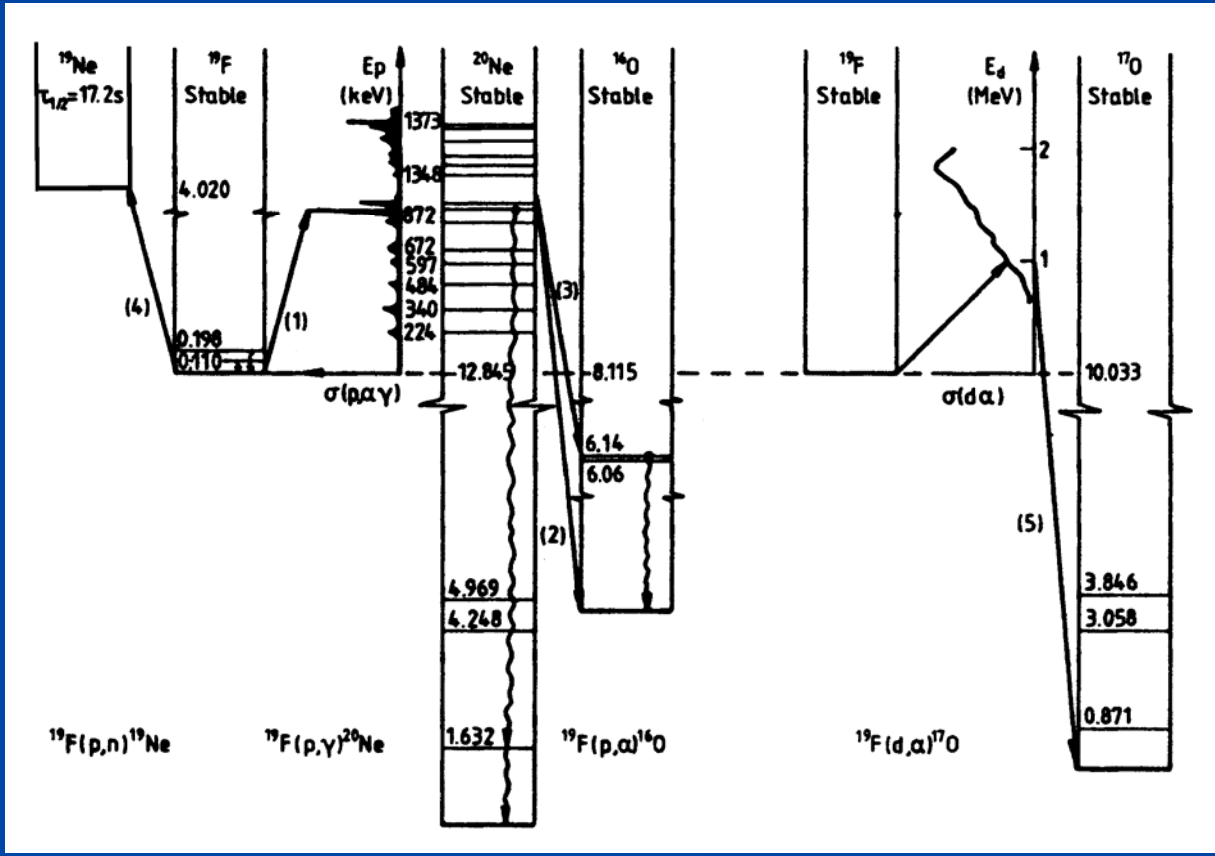

Energy levels and cross sections in nuclear reactions

Natural abundance of stable sotopes

- ^{1}H - 99.985% ^{2}H - 0.015%
- ^{3}He - 0.0001% ^{4}He - 99.999%
- ^{6}Li - 7.56% ^{7}Li - 92.44%
- ^{9}Be - 100%
- ^{10}B - 19.8% ^{11}B - 80.2%
- ^{12}C - 98.89% ^{13}C - 1.11%
- ^{14}N - 99.64% ^{15}N - 0.36%
- ^{16}O - 99.76% ^{17}O - 0.04% ^{18}O - 0.20%
- ^{19}F - 100%
- ^{23}Na - 100%
- ^{24}Mg - 78.99% ^{25}Mg - 10.0 % ^{26}Mg - 11.01%
- ^{27}Al - 100%
- ^{28}Si - 92.23% ^{29}Si - 4.67% ^{30}Si - 3.10%
- ^{31}P - 100%
- ^{50}Cr - 4.35% ^{52}Cr - 83.79% ^{53}Cr - 9.5% ^{54}Cr - 2.36%

Most used particle induced nuclear reactions of light elements

Proton induced reactions	Q [MeV]	Deuteron induced reactions	Q [MeV]	^{3}He induced reactions	Q [MeV]	^{4}He induced reactions	Q [MeV]
$^{6}Li(p,\alpha)^{3}He$	4.02	$^{2}H(d,p)^{3}He$	4.03	$^{2}H(^{3}He,p)^{4}He$	18.35	$^{10}B(\alpha,p)^{13}C$	4.06
$^{7}Li(p,\alpha)^{4}He$	17.35	$^{3}He(d,\alpha)^{1}H$	18.35	$^{6}Li(^{3}He,p)^{8}Be$	6.79	$^{11}B(\alpha,p)^{14}C$	0.78
$^{9}Be(p,\alpha)^{6}Li$	2.13	$^{12}C(d,p)^{13}C$	2.72	$^{9}Be(^{3}He,p)^{11}B$	0.32	$^{14}N(\alpha,p)^{17}O$	-1.19
$^{10}B(p,\alpha)^{7}Be$	1.15	$^{13}C(d,p)^{14}C$	5.95	$^{9}Be(^{3}He,\alpha)^{8}Be$	18.91	$^{19}F(\alpha,p)^{22}Ne$	1.67
$^{11}B(p,\alpha)^{8}Be$	8.58	$^{14}N(d,p)^{15}N$	8.61	$^{12}C(^{3}He,p)^{14}N$	4.78	$^{31}P(\alpha,p)^{34}S$	0.63
$^{15}N(p,\alpha\gamma)^{12}C$	4.97	$^{14}N(d,\alpha)^{12}C$	13.57	$^{12}C(^{3}He,\alpha)^{11}C$	1.86		
$^{18}O(p,\alpha\gamma)^{15}N$	3.98	$^{16}O(d,p)^{17}O$	1.92	$^{18}O(^{3}He,p)^{20}F$	6.87		
$^{19}F(p,\alpha\gamma)^{16}O$	8.11	$^{16}O(d,\alpha)^{14}N$	3.11	$^{18}O(^{3}He,d)^{19}F$	2.50		
$^{23}Na(p,\alpha\gamma)^{24}Mg$	11.69	$^{19}F(d,\alpha)^{17}O$	10.03	$^{18}O(^{3}He,\alpha)^{19}O$	12.51		
$^{27}Al(p,\gamma)^{28}Si$	11.59						
$^{29}Si(p,\alpha\gamma)^{30}P$	5.59						
$^{52}Cr(p,\alpha\gamma)^{53}Mn$	7.56						

Principle

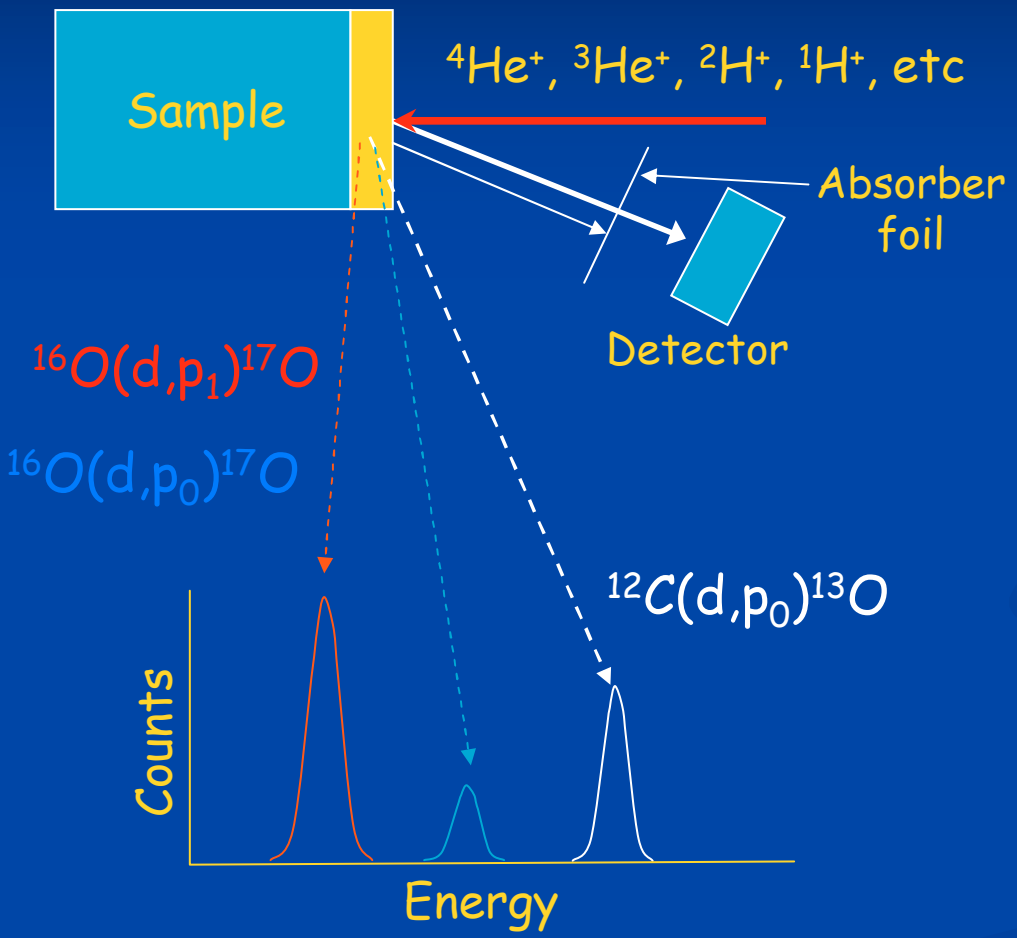
Sample
$^4He^+$, $^3He^+$, $^2H^+$, $^1H^+$, etc
Absorber foil
Detector
$^{16}O(d,p_1)^{17}O$
$^{16}O(d,p_0)^{17}O$
$^{12}C(d,p_0)^{13}O$
Counts
Energy

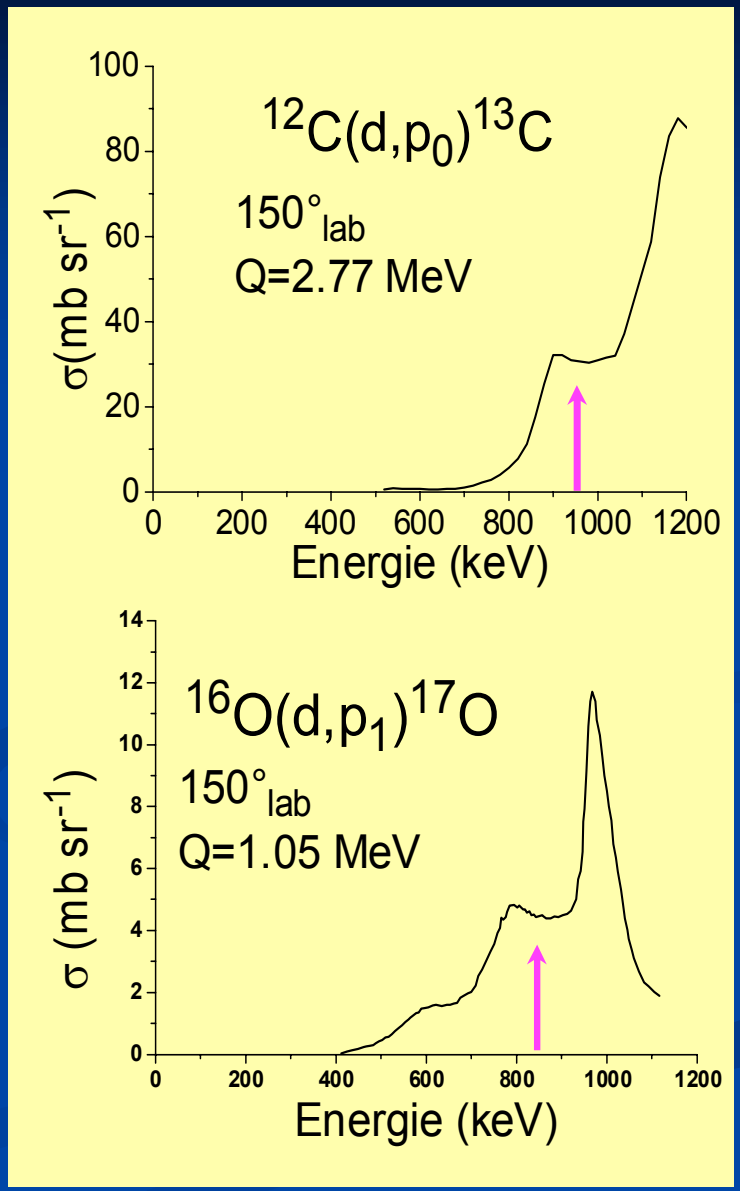
$^{12}C(d,p_0)^{13}C$
150° lab
Q=2.77 MeV
σ(mb sr^{-1})
Energie (keV)
$^{16}O(d,p_1)^{17}O$
150° lab
Q=1.05 MeV
σ (mb sr^{-1})
Energie (keV)

Experimental setup

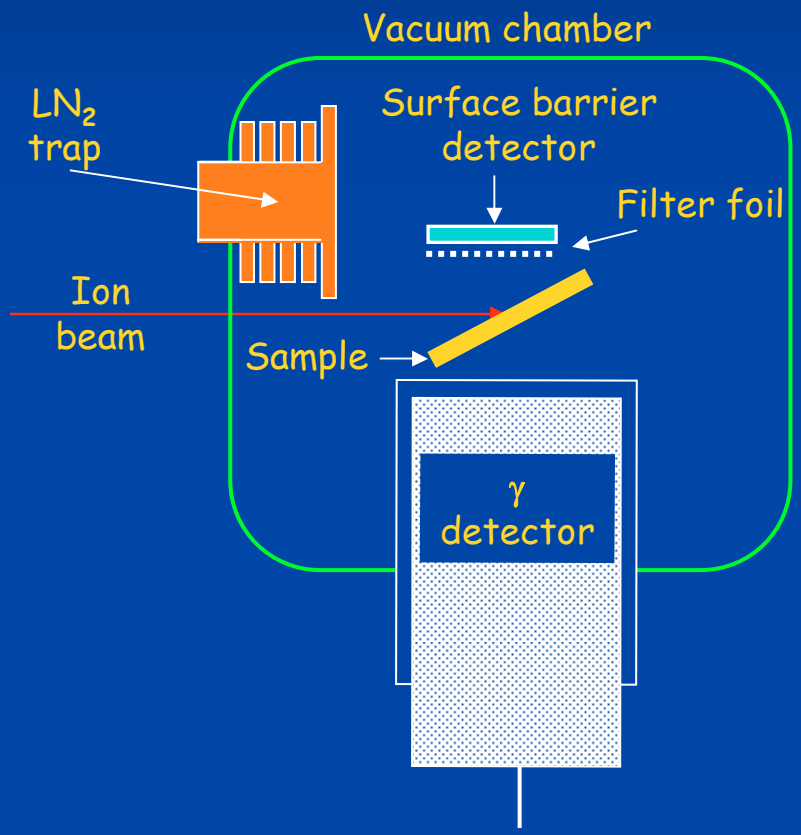

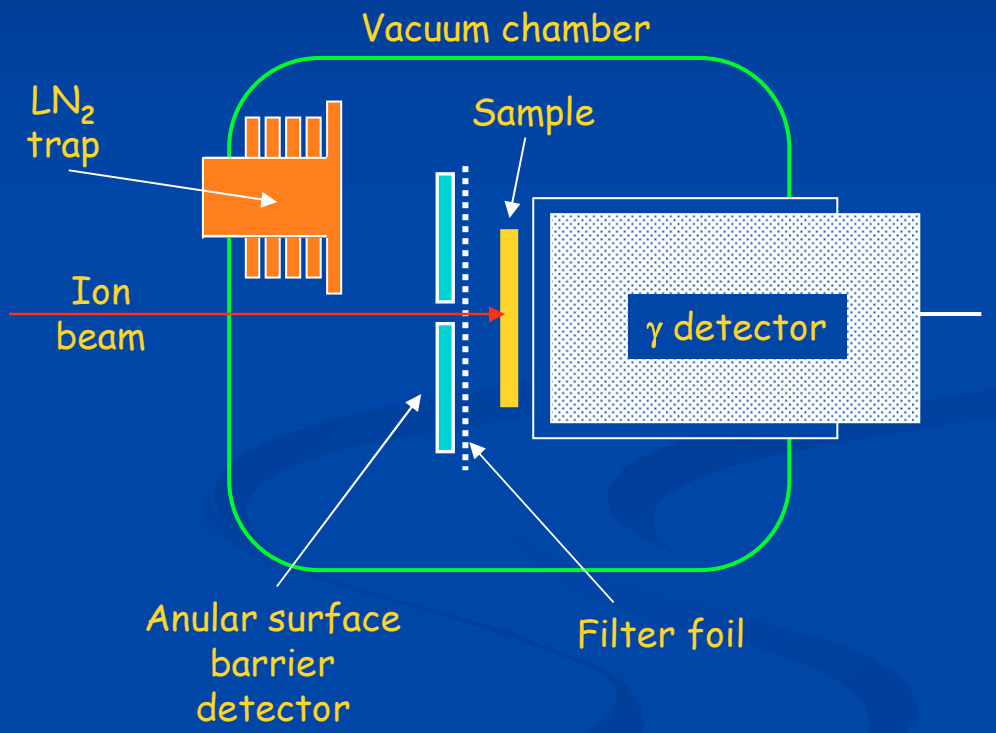

Experimental results

600 nm SiO_2 layer; 900 keV, Deuteron beam

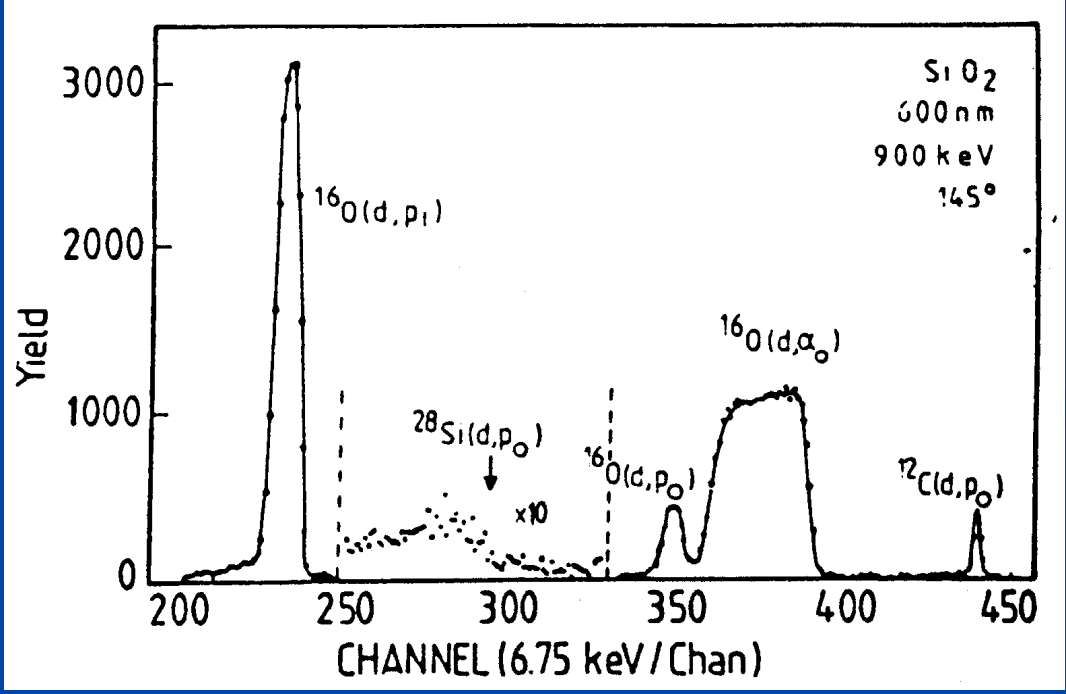

Yield:

$$N_A = \frac{N_b}{\frac{d\sigma(\phi)}{d\Omega} N_a \Delta\Omega}$$

Well known reference sample is needed for quantification !!!

Experimental results

170 nm Al_xN layer, 1.7 MeV d beam

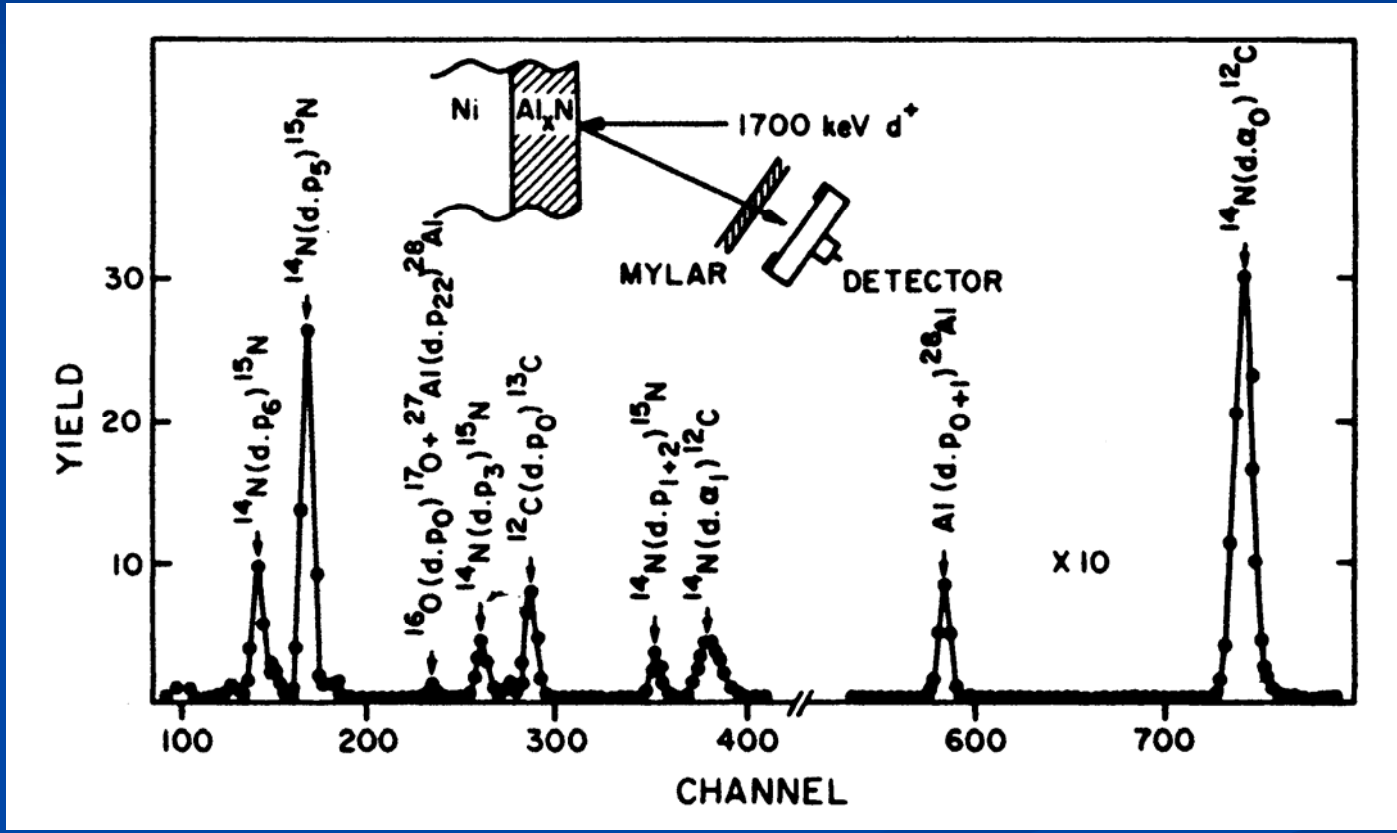

Many reactions, many, sometimes overlapping peaks.
Total amount of the given isotope can be determined.

Thin sample : interferences

900 keV $^{2}H^{+}$ on TiO_xN_y film

Numerous overlapping peaks from $^{14}N(d,p_{0\text{-}7})$ and $^{14}N(d,\alpha_{0,1})$ reactions.

Reaction Q-values are known

In principle, interferences can be accounted for.
In practice we avoid having to.

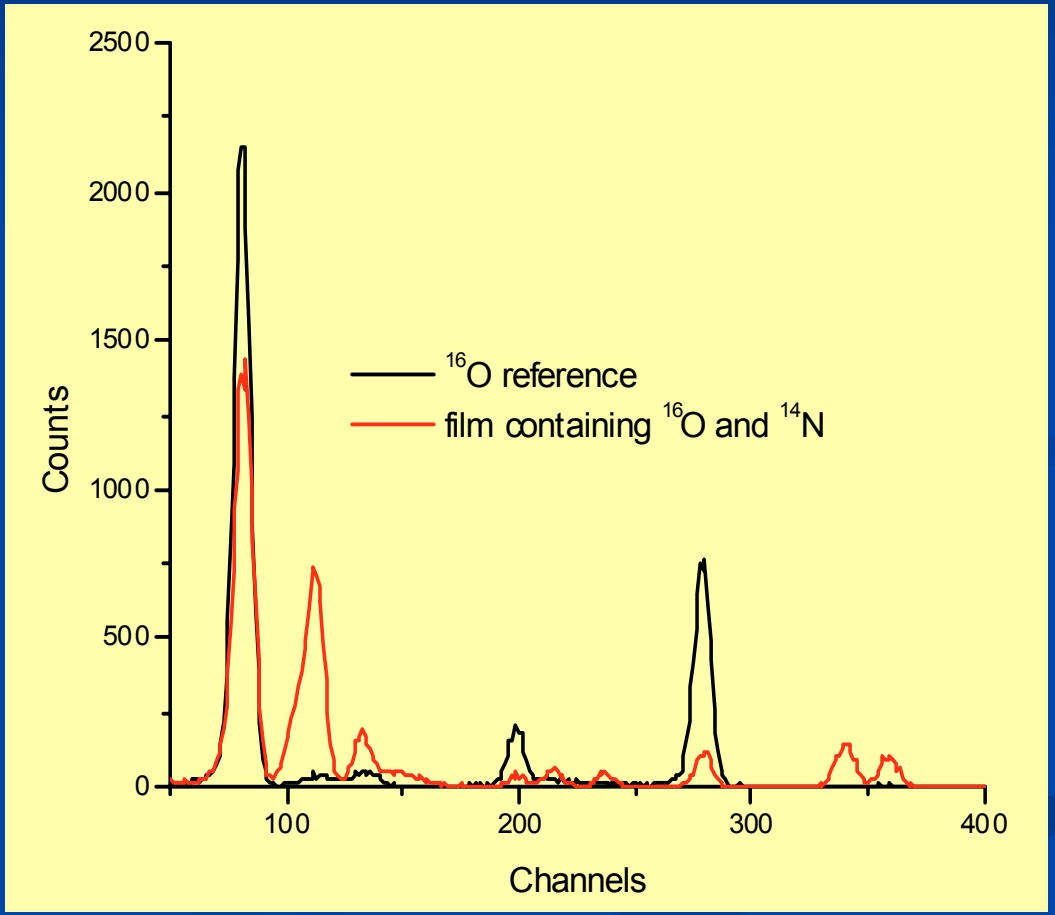

Reference samples

$$N_U = \frac{Y_U}{Y_R} N_R$$

Anodic isotopic Ta_2O_5 thin films for ^{16}O and ^{18}O

Certified ^{16}O and ^{18}O films available from different sources.

For thin targets, the cross section ratios of $^{12}C(d,p)^{13}C$, $D(^3He,p)^4He$, $^{14}N(d,\alpha)^{12}C$, $^{14}N(d,p)^{15}N$, $^{15}N(d,\alpha_0)^{13}C$ and $^{15}N(p,\alpha_0)^{12}C$ to that of $^{16}O(d,p_1)^{17}O$ have been obtained by using stoichiometric frozen gas targets of CO_2, NO and D_2O.

This enables the reliable and robust Ta_2O_5 reference targets to be used as a reference for NRA determinations of D, ^{12}C, ^{14}N and ^{15}N.

Davies, J. A., T. E. Jackman, et al. (1983). "Absolute calibration of $^{14}N(d,\alpha)$ and $^{14}N(d,p)$ reactions for surface adsorption studies." Nucl. Instr. and Meth. 218: 141-146.

Sawicki, J. A., J. A. Davies, et al. (1986). "Absolute cross sections of the $^{15}N(d,\alpha_0)^{13}C$ and $^{15}N(p,\alpha_0)^{12}C$ reaction cross sections." Nucl. Instr. and Meth. B15: 530-534.

Depth Profiling : Principle

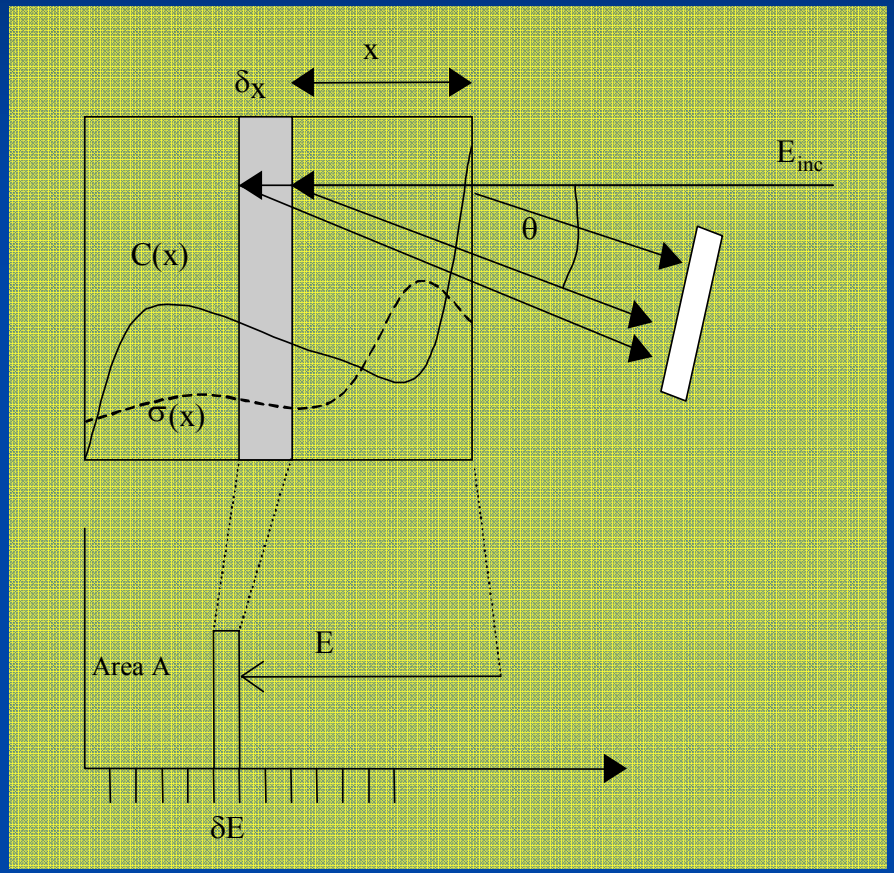

- A channel of width dE_c at energy E_c in the spectrum corresponds to a slice of width dx at depth x in the sample, with E_c and dE_c being inversely related to x and dx through a linear combination of the stopping powers for the incident and outgoing particle
- The number of particles accumulated into that histogram bin is proportional to C(x), dx, and $\sigma(E_x)$, where E_x is the energy of the incident beam when it gets to depth x;

$$Y = N\sigma(E)$$
$$= C\Delta x\sigma(E)$$
$$= \int_{\Delta x} C(x)\sigma(E)dx$$

Depth profiling

Depth profiling nitrogen in titanium via $^{14}N(d,\alpha_1)^{12}C$

Cross section

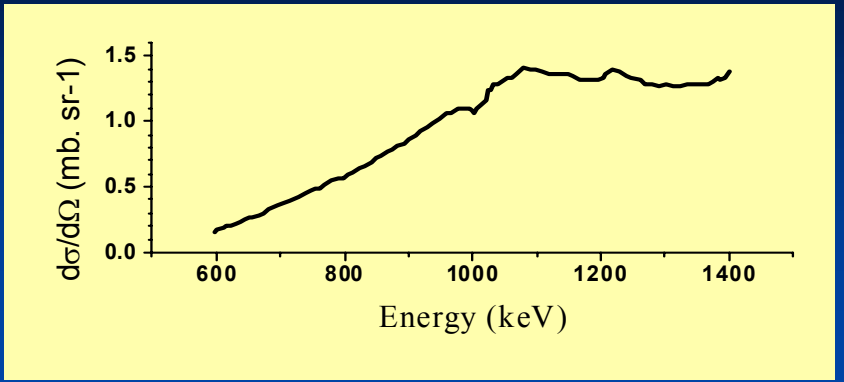

Spectra

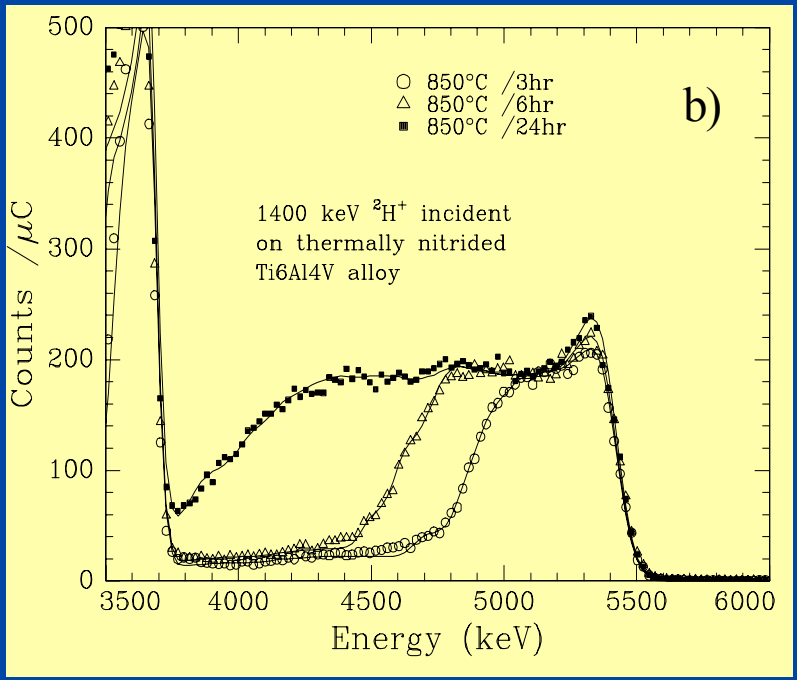

Concentration profile

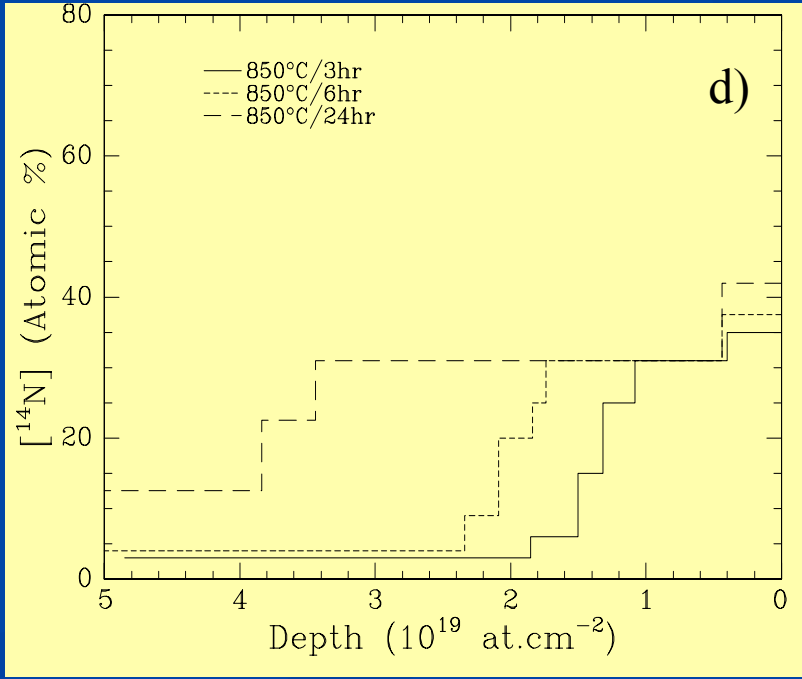

Ion implantation of SiC

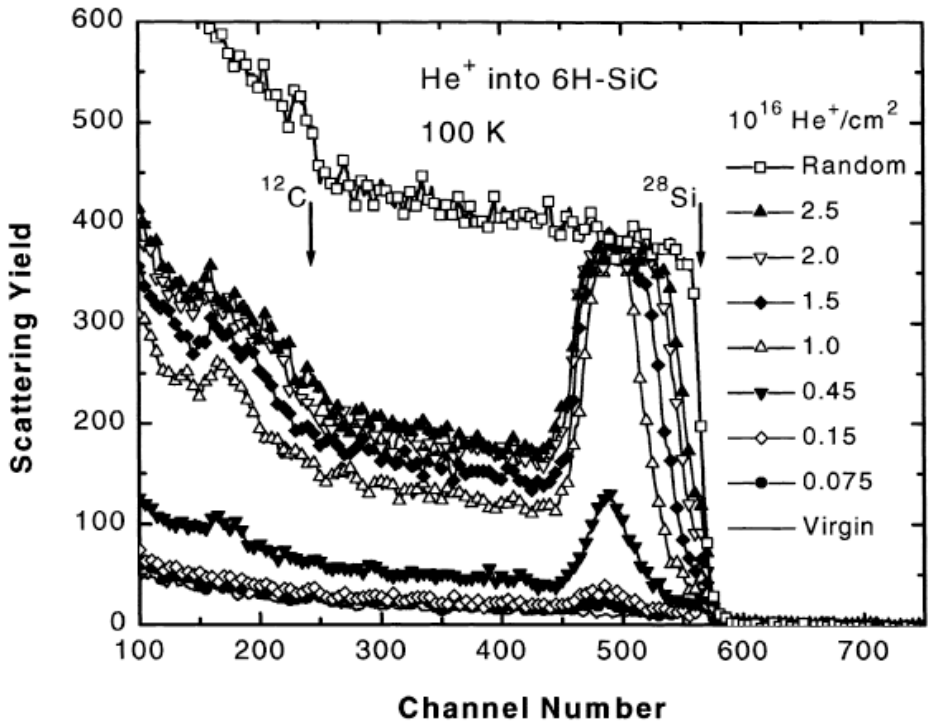

Fig. 1. A sequence of 2.0 MeV He^+ RBS/C spectra taken at room temperature for ⟨0001⟩-oriented 6H–SiC wafers implanted at 100 K with 50 keV He^+ ions. Also included are a random-equivalent spectrum and a channeling spectrum from a virgin area.

RBS + channeling = lattice disorder

RBS + NRA = More information

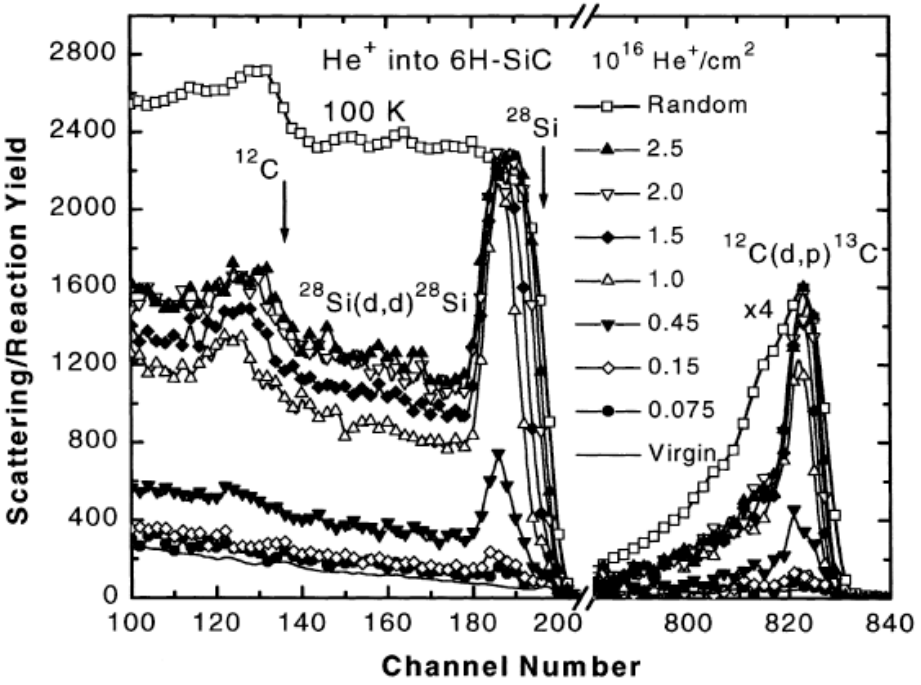

Fig. 2. A sequence of 0.94 MeV D^+ RBS/C and NRA/C spectra taken at room temperature for the same sample as in Fig. 1.

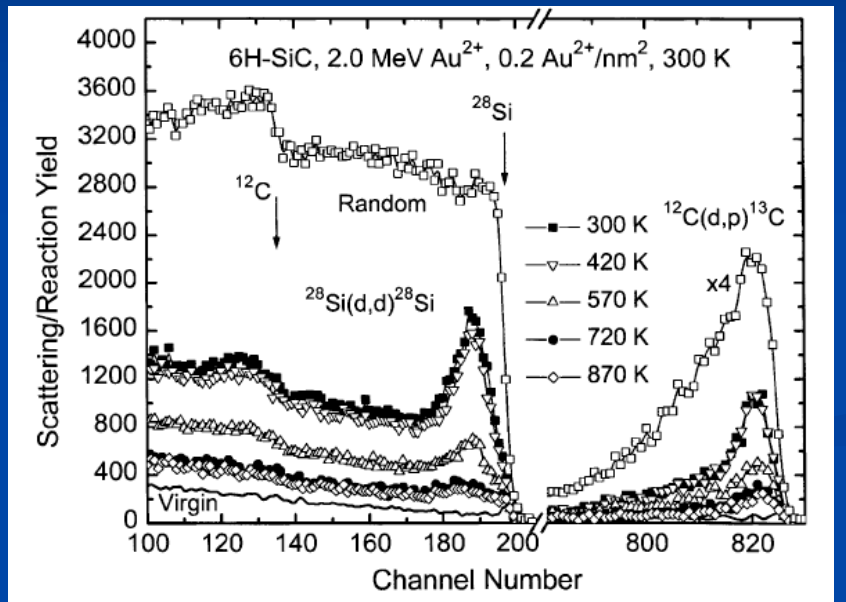

Fig. 5. A sequence of in situ 0.94 MeV D^+ RBS and NRA channeling spectra for ⟨0 0 0 1⟩-oriented 6H–SiC wafers irradiated 60° off surface normal at 300 K to an ion fluence of 0.2 Au^{2+}/nm^2 and annealed at successively higher temperatures for 20 min each. Also included are random-equivalent and channeling spectra from a virgin area.

W. Jiang et al. / Nucl. Instr. and Meth. in Phys. Res. B 161±163 (2000) 501

Thin sample : summary

- dE/dx not needed
- Shape of $\sigma(E,\theta)$ much more important than absolute value. Precision standards are used rather than precision cross sections (Standardless NRA?)
- Approximate *relative* cross sections are needed to help in experimental design (isotopes …)
- Reaction Q values are needed - these are easily accessible and well known.

Resonances

$^{18}O(p,\alpha)^{15}N$ cross section

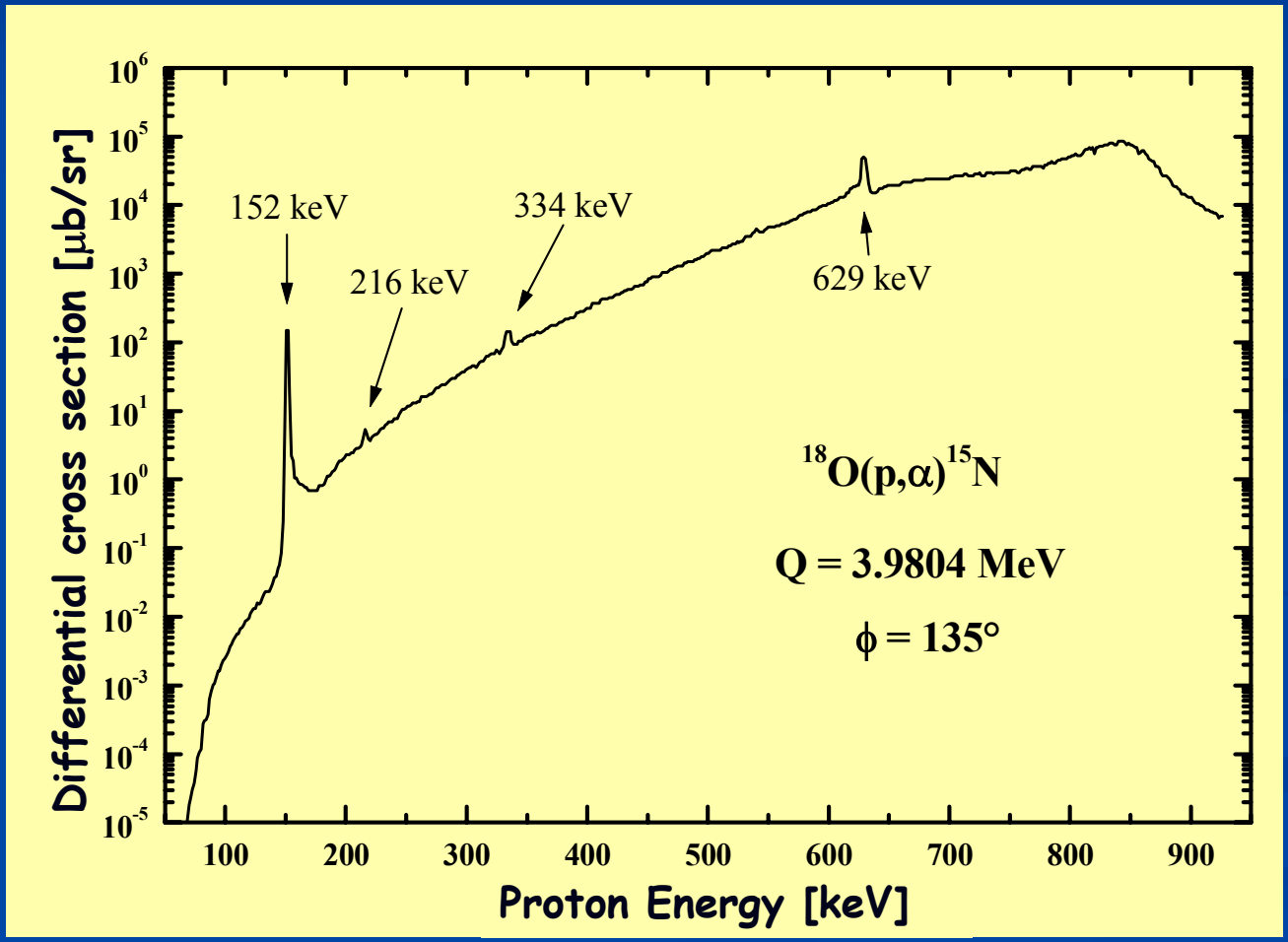

Cross section in the resonance: Breit-Wigner (Lorenz) function

$$\sigma_R(E) = K \frac{\Gamma^2}{(E - E_R)^2 + \frac{\Gamma^2}{4}}$$

Most used Narrow Resonances in Depth Profiling

Reaction	Resonance energy	Resonance width
$^{18}O(p,\alpha)^{15}N$	152 keV	100 eV
$^{29}Si(p,\gamma)^{30}P$	413.9 keV	
$^{15}N(p,\alpha)^{12}C$	429 keV	120 eV
$^{30}Si(p,\gamma)^{31}P$	620.4 keV	68 eV
$^{18}O(p,\alpha)^{15}N$	629 keV	2000 eV
$^{27}Al(p,\gamma)^{28}Si$	632.23 keV	6.7 eV
$^{23}Na(p,\gamma)^{24}Mg$	676.7 keV	<70 eV
$^{27}Al(p,\gamma)\ ^{28}Si$	991.86 keV	70 eV
$^{52}Cr(p,\gamma)^{53}Mn$	1005 keV	50 eV
$^{13}C(p,\gamma)^{13}N$	1748 keV	135 eV

Depth Profiling by Resonance

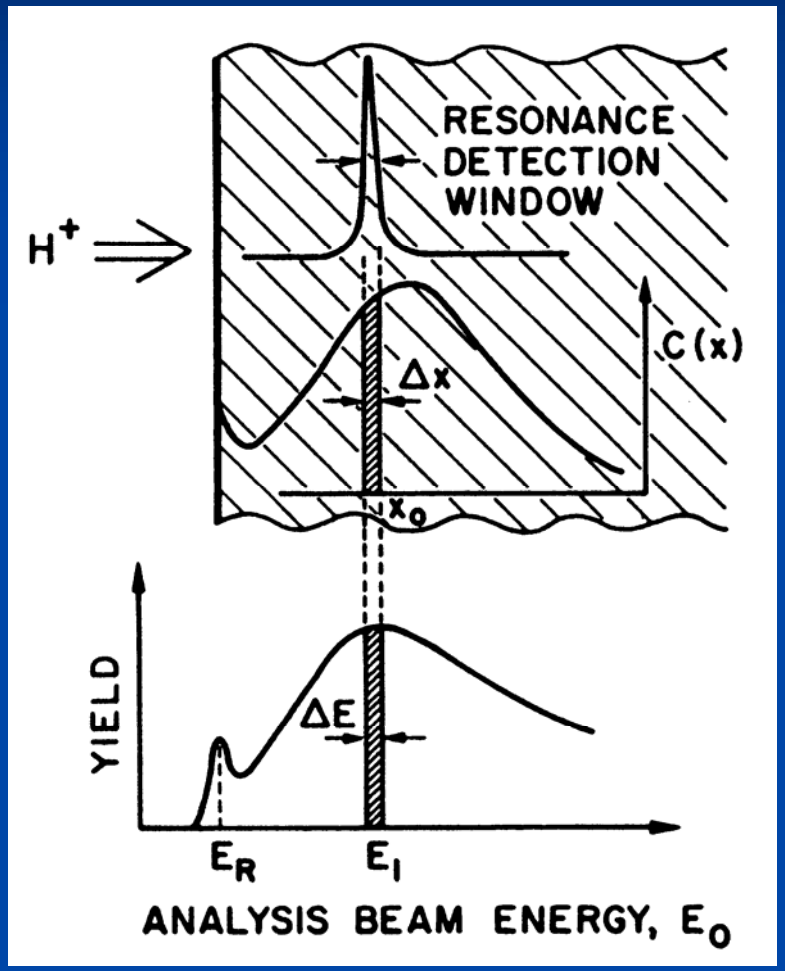

The resonance is scanned through the target depth by scanning the incident beam energy.

Resonance samples the given isotope at depth

$$x = \frac{E_0 - E_R}{\frac{dE}{dx}}$$

Principle of depth profiling with narrow resonances

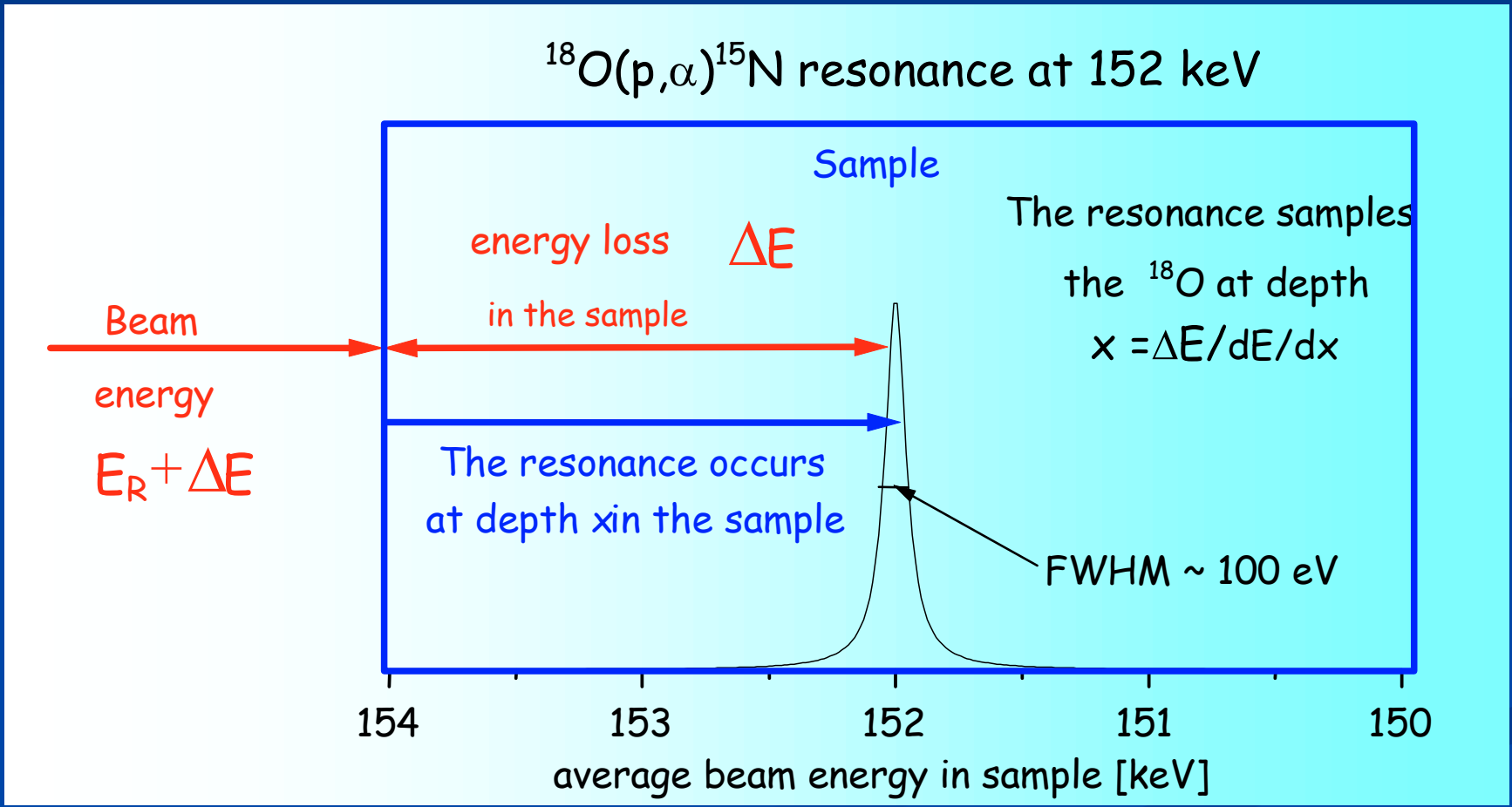

An excitation curve

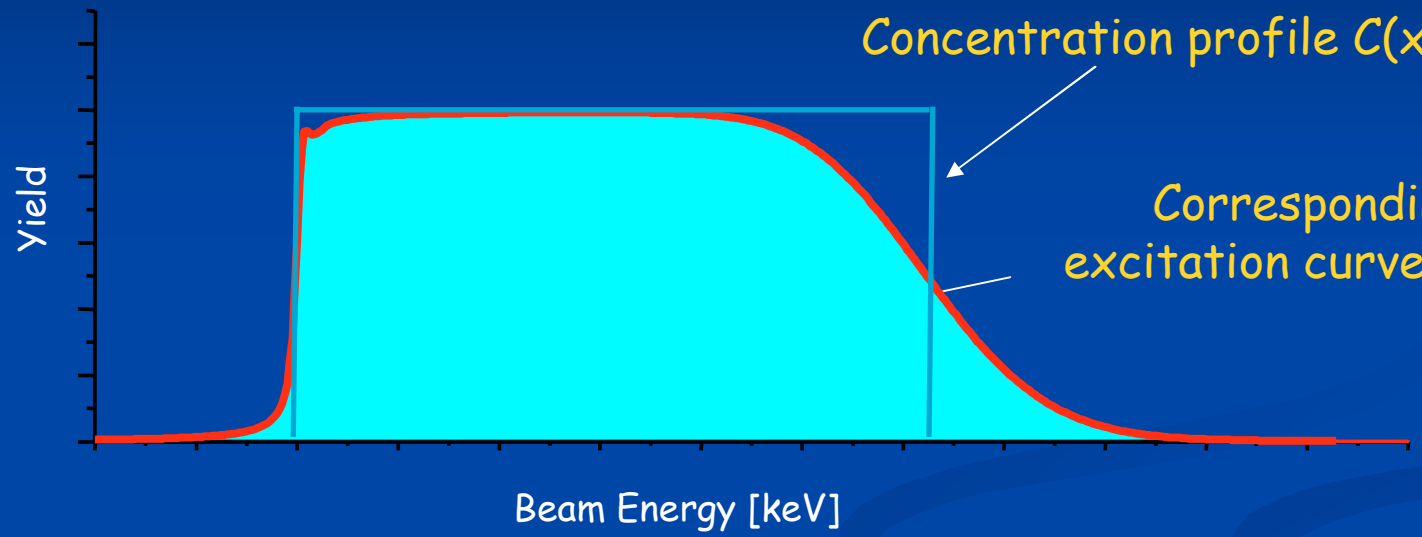

$$N(E) = G(E) * \Gamma(E) * T(E) * S\langle C(x)\rangle$$

$$S\langle C(x)\rangle = \sum_{n=0}^{n=\infty} k_n f^{*n}(u)$$

$G(E)$	beam + Doppler energy spread
$\Gamma(E)$	rersonance lineshape
$T(E)$	beam energy straggling
$S\langle C(x)\rangle$	„straggling" of C(x)

Excitation curve

$G(E)$ beam - Gaussian,
+ Doppler energy spread due to the thermal vibration of the target atoms

$$\sigma_D^2(E) = \frac{2M_A E}{M_a} kT$$

$\Gamma(E)$ rersonance lineshape - Lorantzian

$$\sigma_R(E) = K \frac{\Gamma^2}{(E - E_R)^2 + \frac{\Gamma^2}{4}}$$

$\Omega(E)$ beam energy straggling

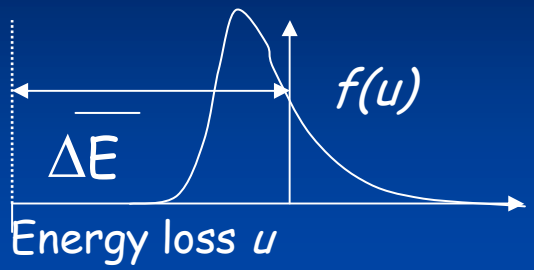

The charged particles lose their energy in independent collisions with electrons.

$f(u;x)$ tends towards a Gaussian for large x

$$\sigma(f(u)) = S\sqrt{\frac{2Z}{A}}\sqrt{x}$$

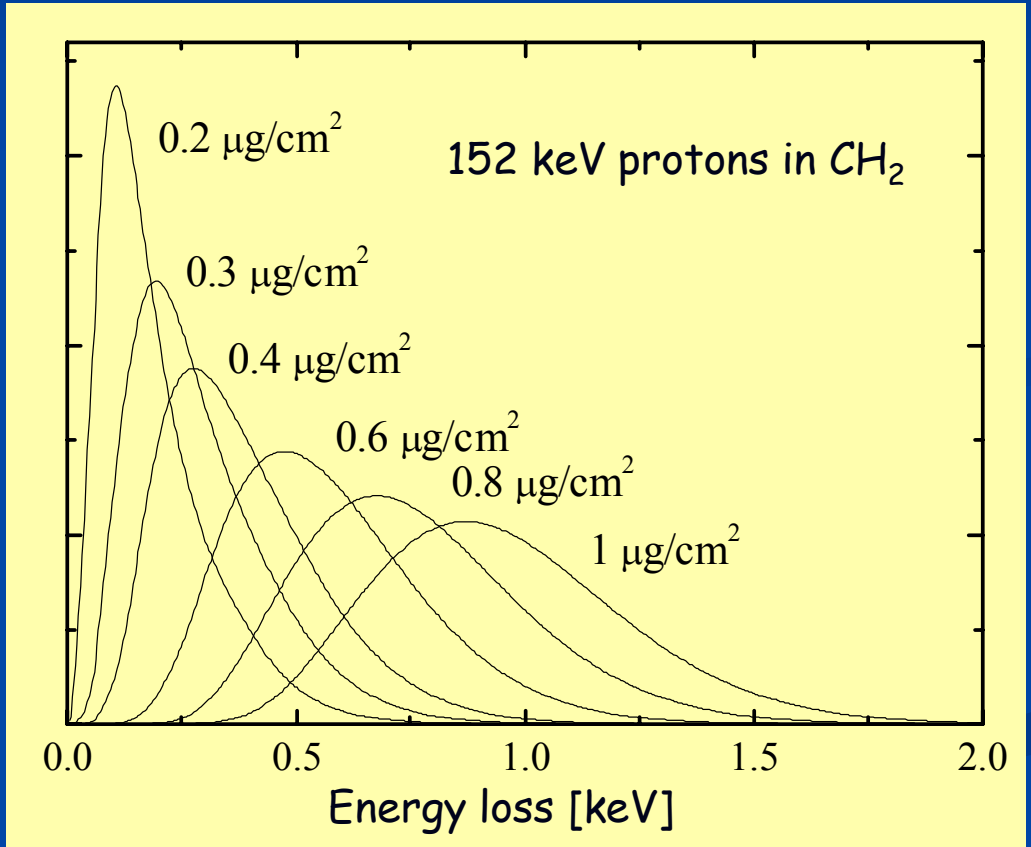

„Straggling"

S<C(x)> 'straggling' of C(x)

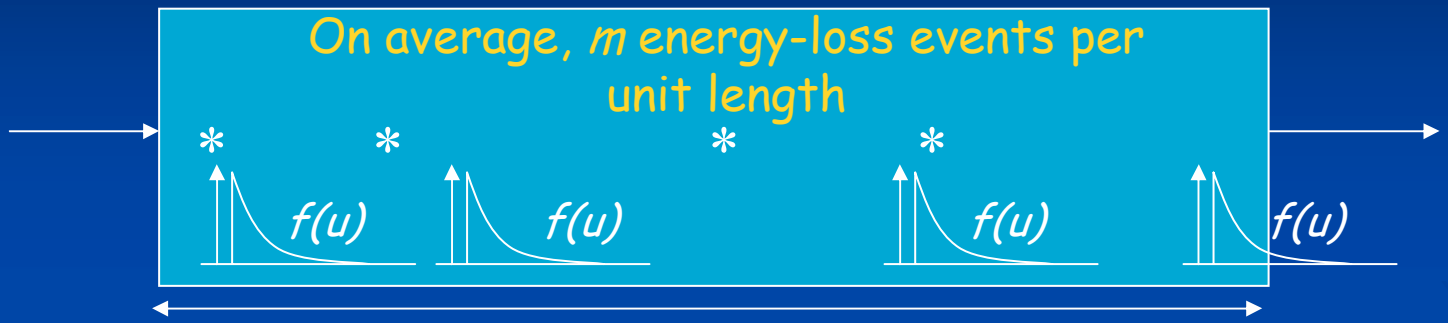

For thickness x mx events on average

$$g(u;x) = \sum_{n=0}^{n=\infty} P_n(mx) f^{*n}(u)$$

$$P_n(mx) = e^{-mx} \frac{(mx)^n}{n!}$$

Experimental excitation curves

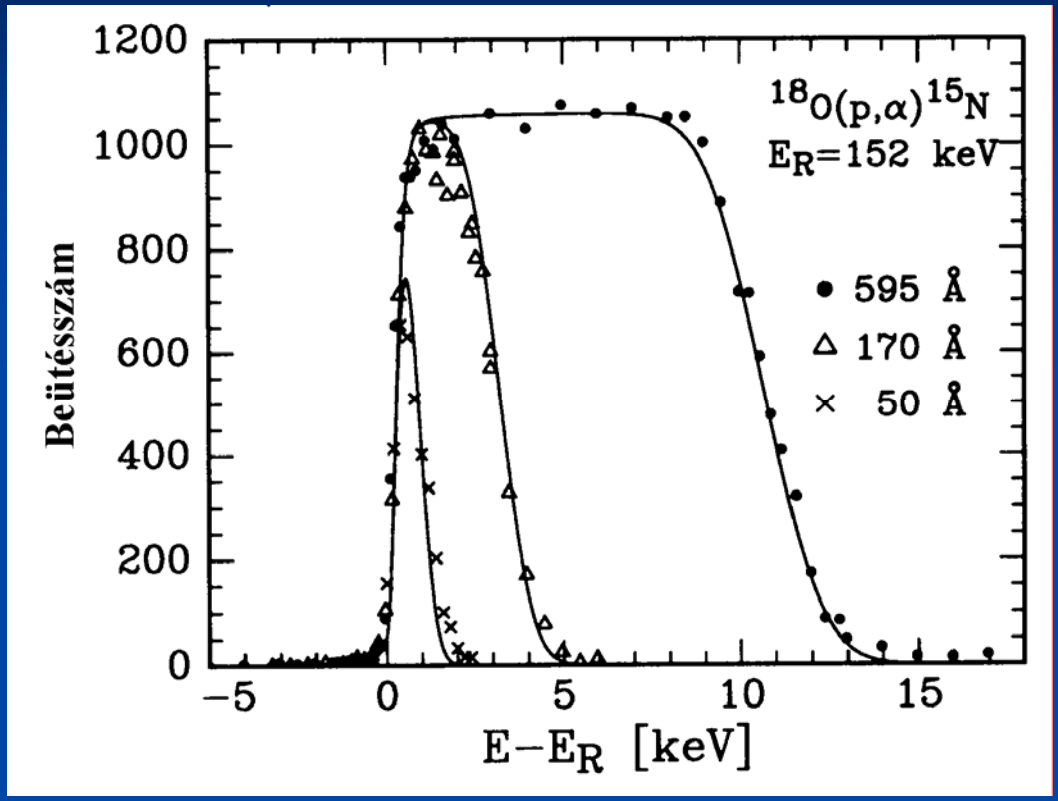

$Si^{18}O_2$ /Si sample, thermally grown, 20 μC /point

Beam energy spred + Doppler broadening: 100 eV

Resonance width: 100 eV

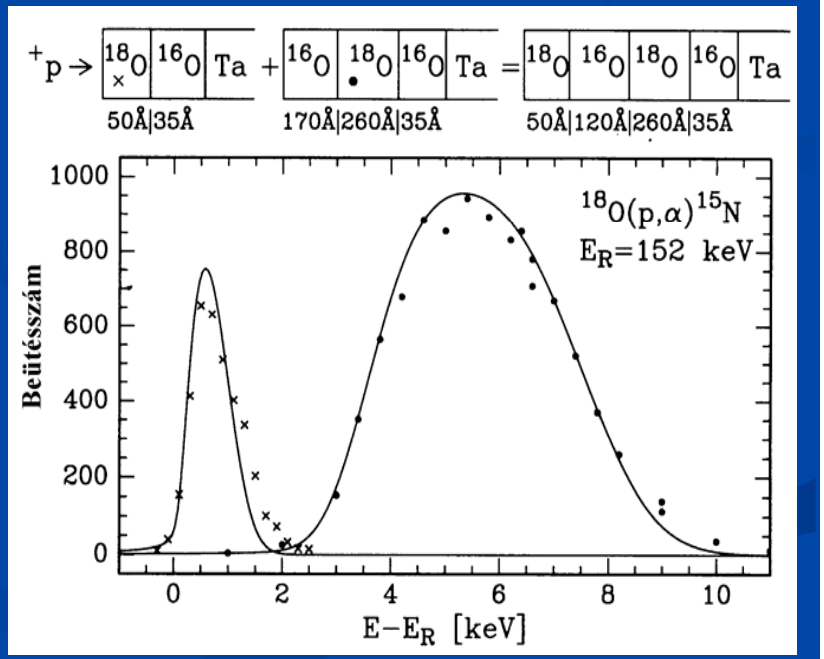

$Ta_2{}^{18}O_5$ /Ta sample, anodically oxidised, 20 μC /point

Tilting the sample – increases the virtual thickness of the layer

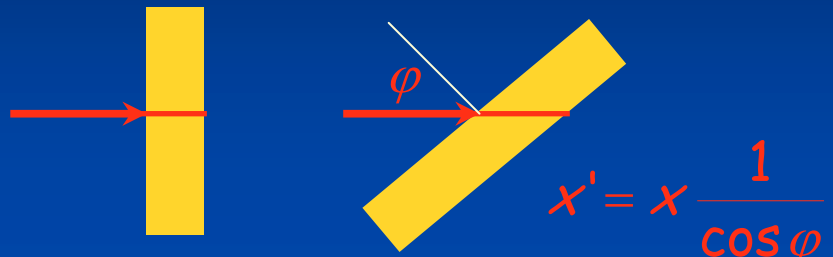

$$x' = x \frac{1}{\cos\varphi}$$

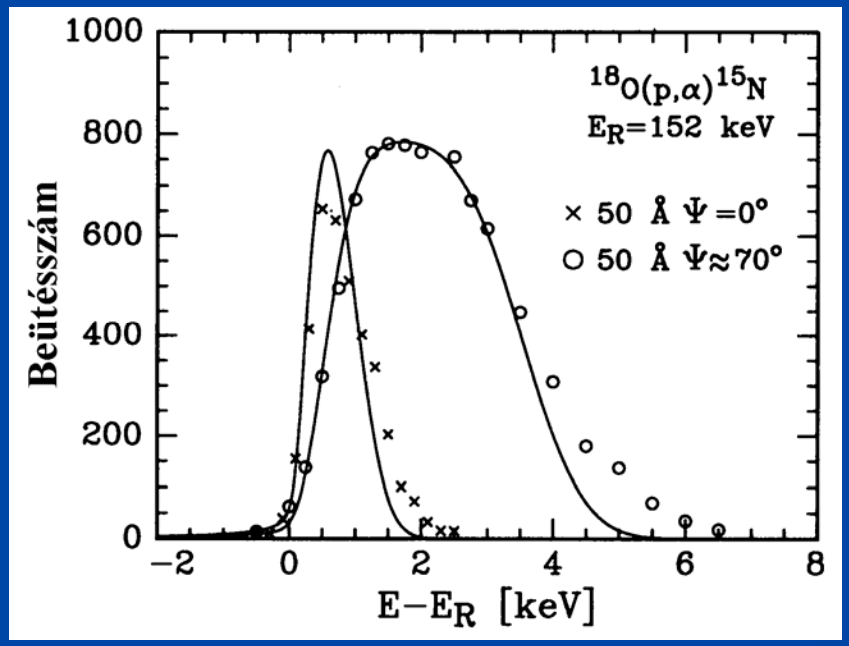

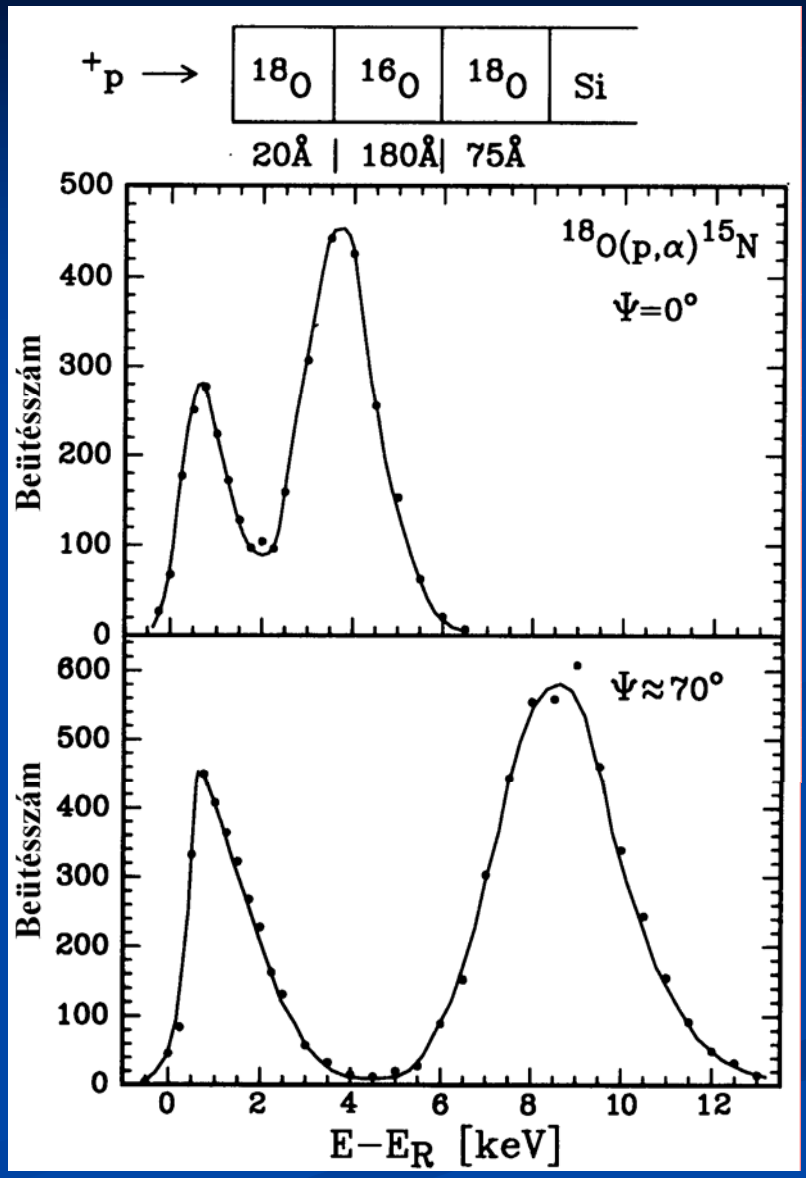

Depth resolution

+

- Narrow resonance width
- Large dE/dx (~ 100 keV)
- „negligible cross section outside the resonance – Background-free

–

- Straggling – beam broadens by depth
- Multiple Scattering at tilted sample

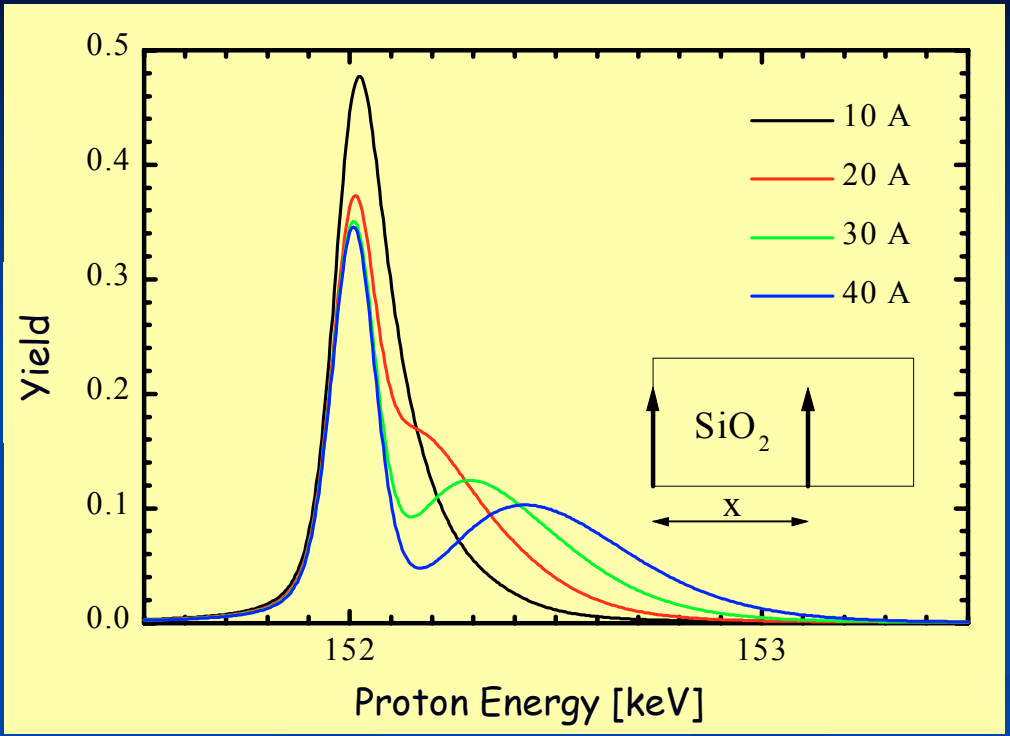

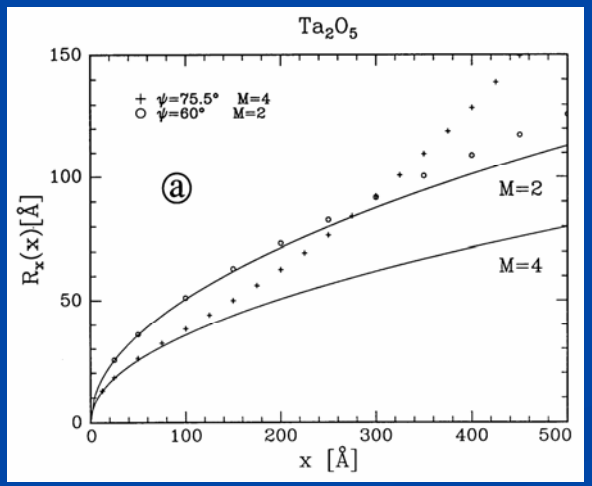

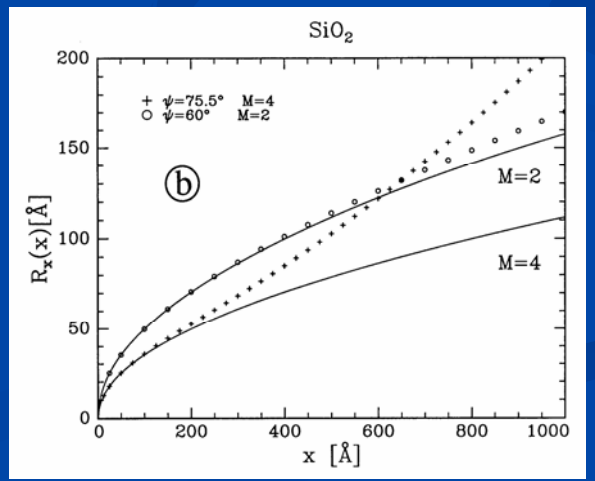

Depth resolution vs Depth

ψ: tilt angle
line: straggling
circles: MS
crosses: overall

Depth Profiling by Resonance - Summary

- As for thin samples, plus need for accurate S(E)
- low energy – large stopping – high depth resolution
- Stronger requirement for shape accurate $\sigma(E,\theta)$ for accurate depth profiling
- Straggling and Multiple scattering gradually decreases resolution

Typical experimental results

Isotopic tracing study of the microscopic mechanisms of oxygen transport in the oxide growing during dry oxidation of silicon.

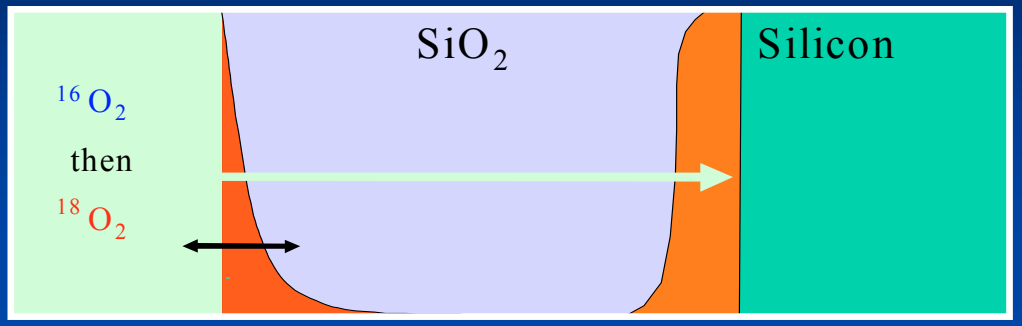

^{18}O depth profile Experimental excitation curve

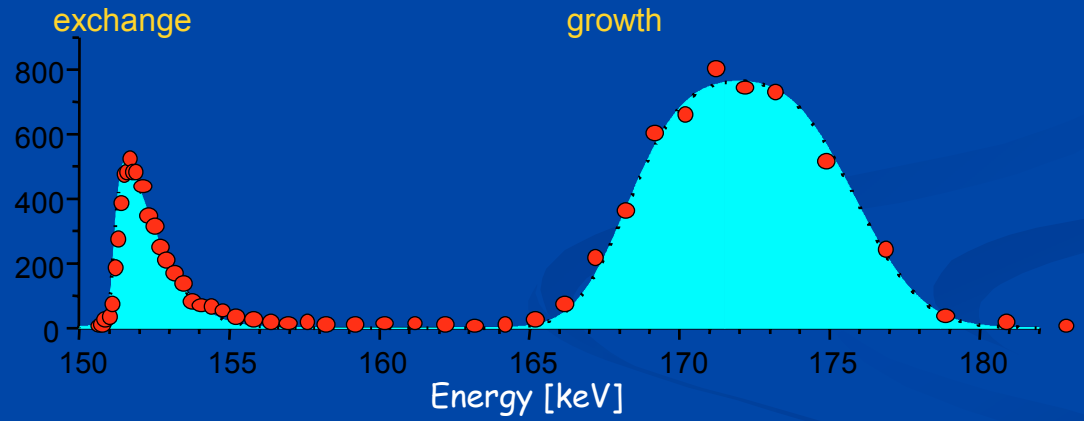

Interpretation of the spectra in terms of ^{18}O depth profile, demonstrating surface exchange and that the growth takes place at the SiO_2/Si interface through interstitial oxygen movement: direct confirmation of the Deal and Grove model for growth $x > 10$ nm.

No isotopic exchange in the matrix (natural abundance, 0.2%) except near the surface.

^{18}O depth profile

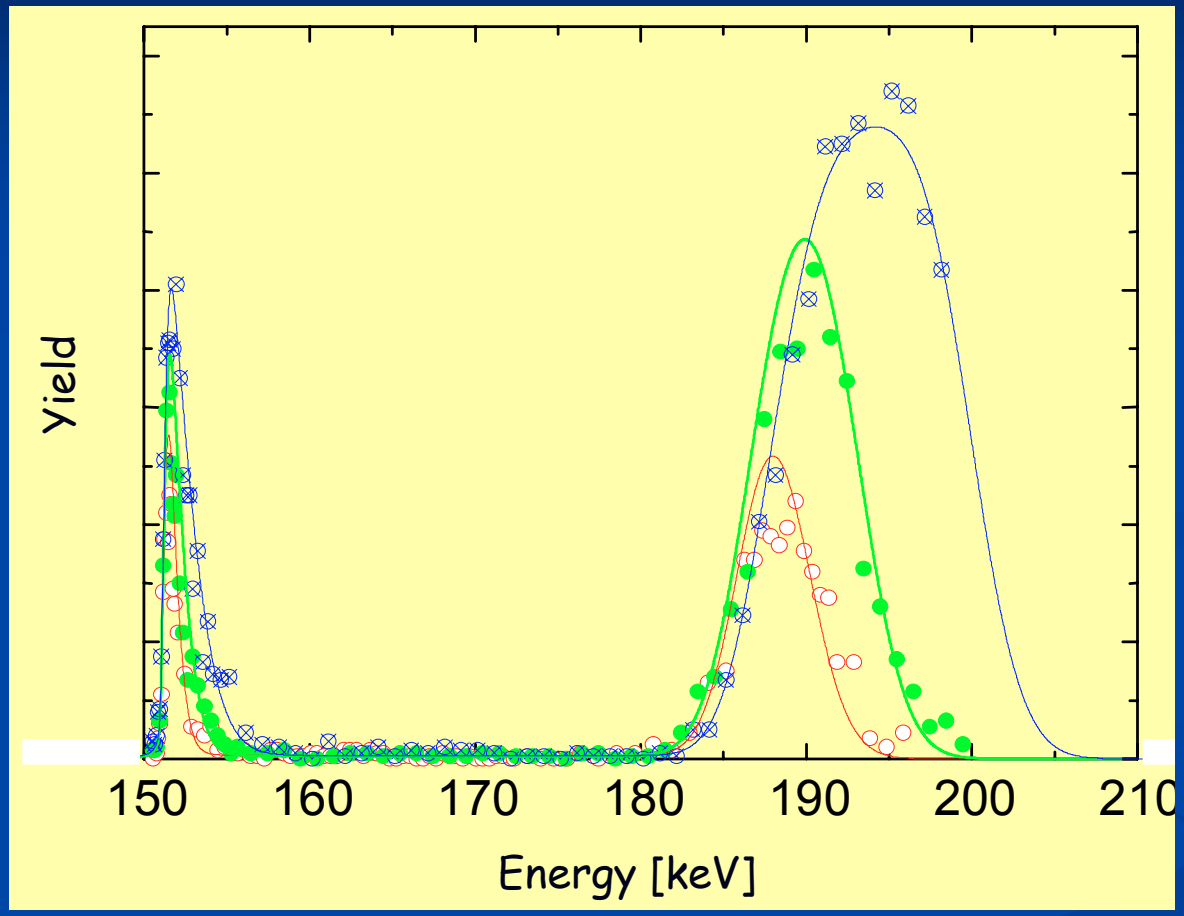

Sequential oxidations in 100 mb $^{16}O_2$ (40 h) at 1100°C, yielding 1600 Å $Si^{16}O_2$ then in $^{18}O_2$ (5 h, 10 h and 24 h: additional 100, 285 and 405 Å). Excitation curve registration with target tilted to 60°.

I. Trimaille et al. GPS, Paris

Isotopic tracing by sequential oxydation of SiC

$^{16}O_2$ (40 h) then $^{18}O_2$ (5 h, 10 h and 24 h)

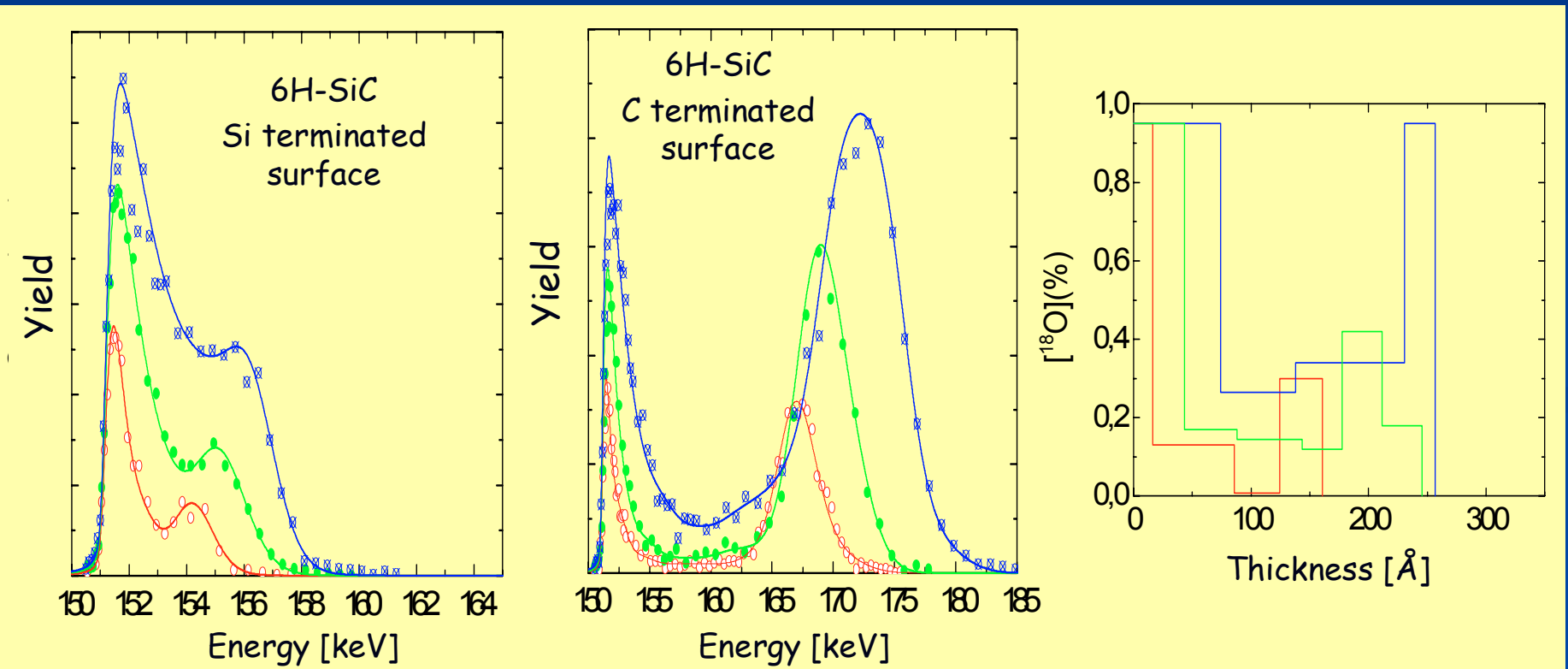

Sequential $^{16}O_2/^{18}O_2$ oxidations, same conditions as for Si. SiC is a polar crystal: silica grows on both faces, similarly to the Si case, but the Si and C faces produce slow and fast growth. Isotopic tracing measurements of this type allow one to investigate with great sensitivity the near surface and interface properties of the silica produced by oxidation of SiC.

Hydrogen profiling with a nuclear resonance

$^{1}H(^{15}N,\alpha\gamma)^{12}C$

Hydrogen implantation profile in silicon (10^{16} cm^{-2}, 40 keV)

from W.A. Lanford, NIMB66(1992),68

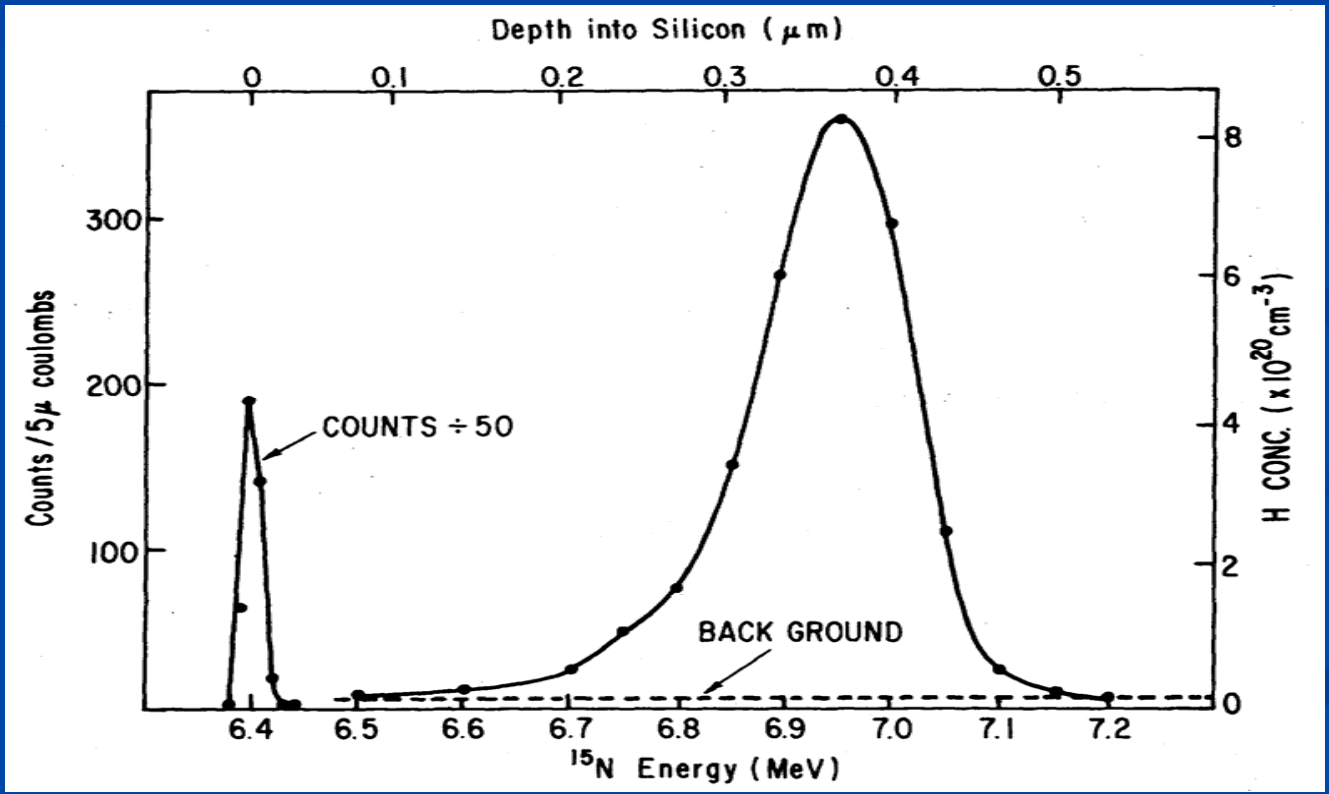

Study of thin hafnium oxides deposited by atomic layer deposition

J.-J. Ganem, NIM B 219–220 (2004) 856

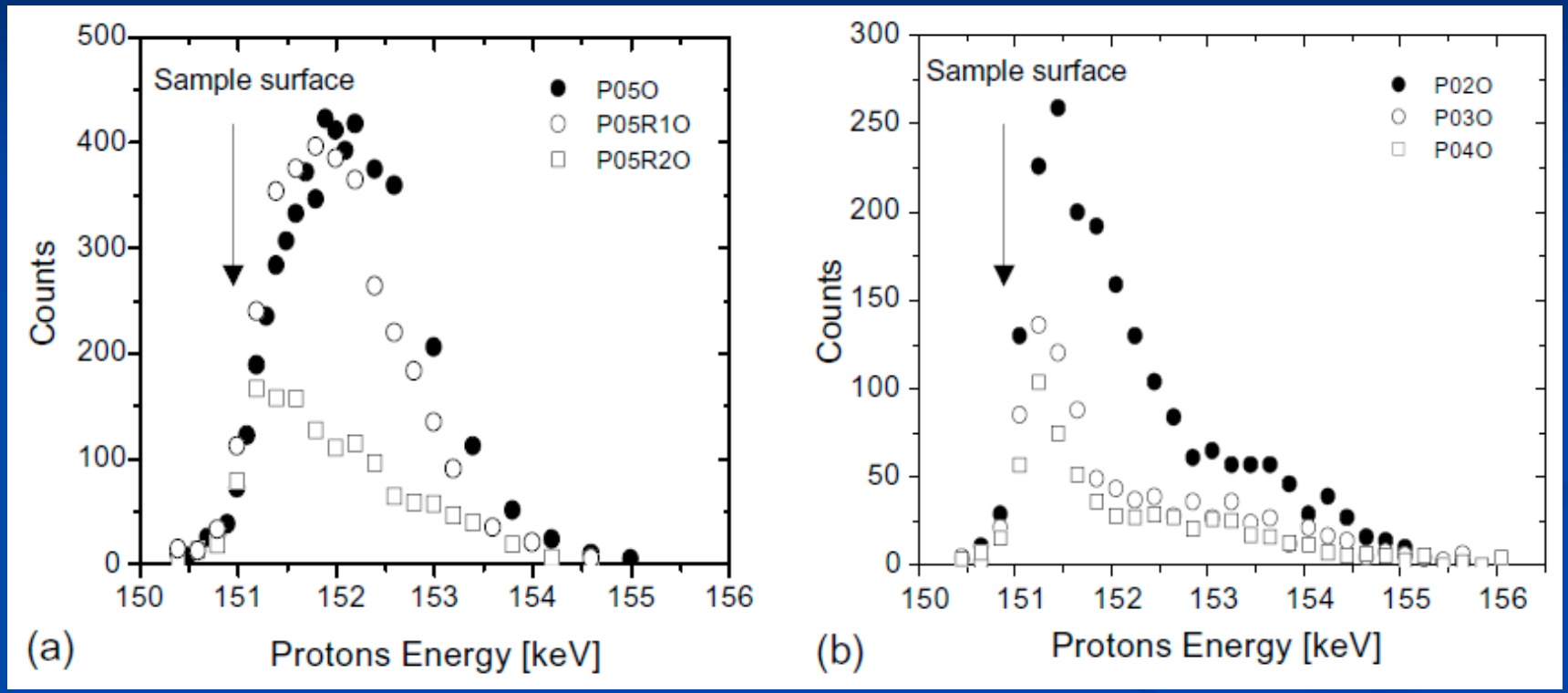

Excitation curves measured using the 151 keV $^{18}O(p;\alpha\chi)^{15}N$ resonance on 3.5 nm (a) and 7.5 nm (b) HfO_2 samples oxidized in $^{18}O_2$ atmosphere at 425 C just after: deposition (black circles), post-deposition N_2 anneal at 425 C (open circles) and post-deposition N_2 anneal at 800 C (open squares).

After deposition the films present chlorine contamination and a lack of oxygen. They are unstable toward thermal oxidation since a high oxygen transport and exchange mechanisms occur during the process. Oxygen diffusion can be significantly reduced after a thermal anneal in N_2 atmosphere.

Ultrathin silicon oxynitride film formation

Experimental excitation curves of the $^{18}O(p,\alpha)^{15}N$ reaction for samples with (a) deferent ^{15}N areal densities, sequentially oxidized in $^{16}O_2$ (60 min) and in $^{18}O_2$ (90 min). The arrows indicate the energy position of the surface (dashed) and of the SiO_2/Si interface (solid) in each sample; (b) no N prior to oxidation, oxidized under the same conditions as samples in (a).

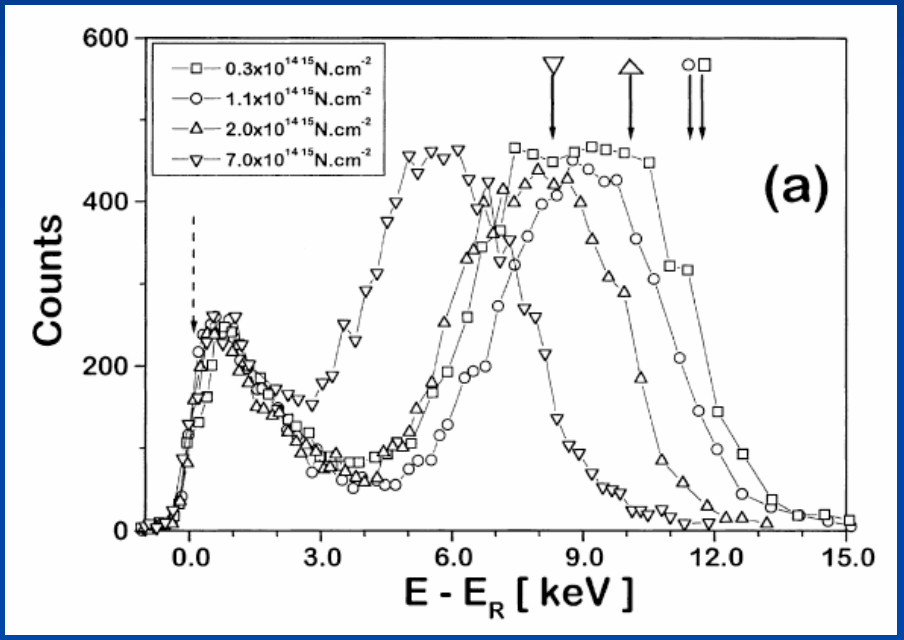

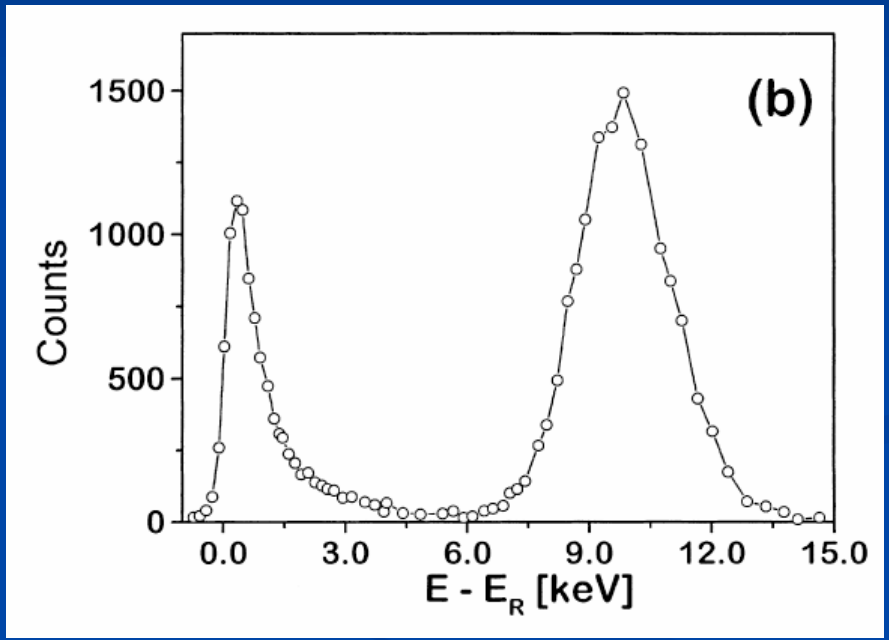

(i) N amounts as low as 1/30 of a monolayer at the surface of Si wafers hamper the oxidation of Si, and the higher the N concentration, the thinner the oxynitride films;

(ii) (ii) during the film growth, N and O are responsible for the atomic transport, while Si remains immobile;

(iii) N, which is initially present at the surface of the Si wafer, migrates during oxidation, remaining at the near-surface and at the near-interface regions of the film.

Silicon isotopic tracing with the $^{29}Si(p,\chi)$ narrow resonance near 415 keV

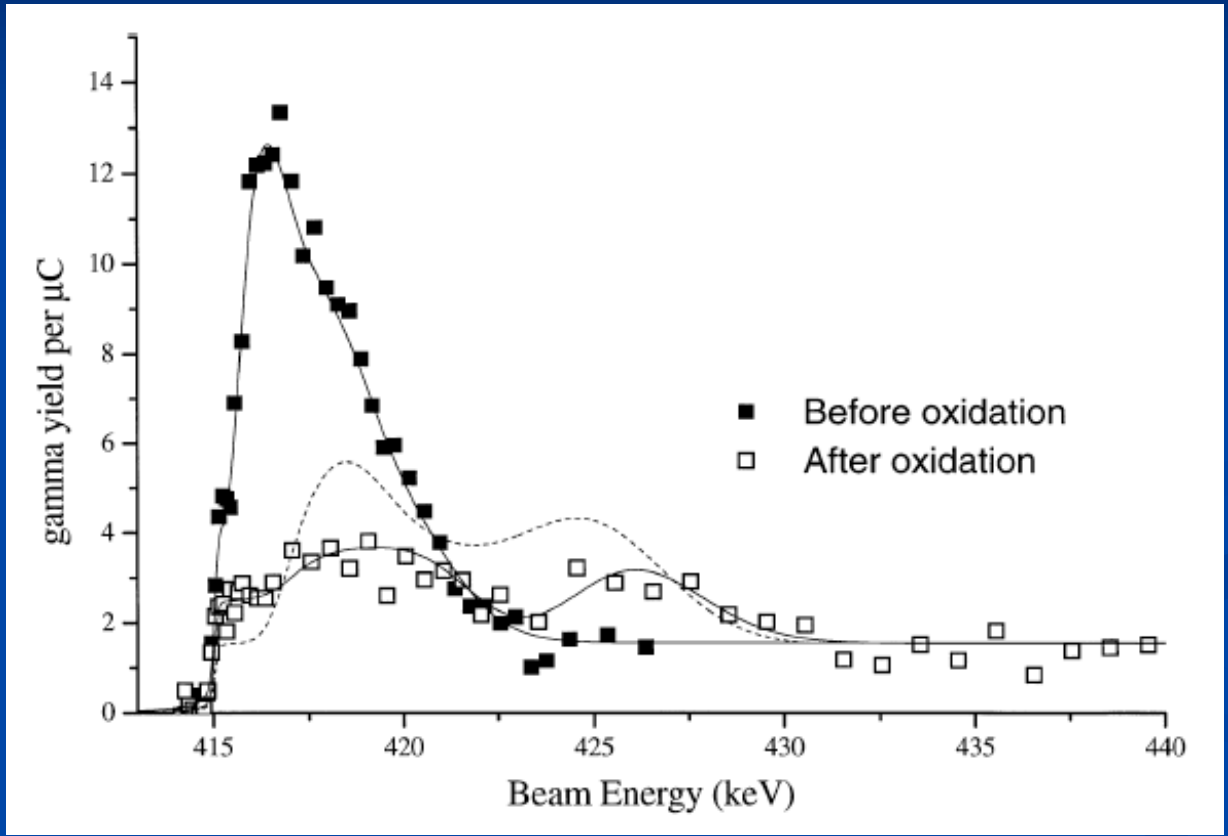

$^{29}Si(p, \chi)^{30}P$ excitation curves from an enriched silicon single crystal before and after thermal oxidation, showing loss of silicon during the oxidation process.

I.C. Vickridge et al, NIM B 161±163 (2000) 441

Annealing of $ZrAl_xO_y$ Ultrathin Films on Si in a Vacuum or in O_2

E. B. O. da Rosa et al., Journal of The Electrochemical Society, 148 G695-G703 (2001)

$ZrAl_xO_y$ films were deposited at a rate of 0.3 nm/min by reactive sputtering using a Zr_{80}-Al_{20} atomic composition target in an oxygen-containing plasma directly on Si(001) substrates. Postdeposition annealings were performed ex situ at 600°C for 10 min, either in high vacuum ($p \approx 10^{-5}$ Pa) or in 7×10^{-3} Pa of dry 98.5% $^{18}O_2$.

Areal densities of Al and Si were estimated from the areas of the excitation curves of the $^{27}Al(p,\gamma)^{28}Si$ and $^{29}Si(p,\gamma)^{30}P$ nuclear reactions around the resonance energies at 404.9 and 414 keV. The as-deposited film has an approximate composition Zr_4AlO_9.

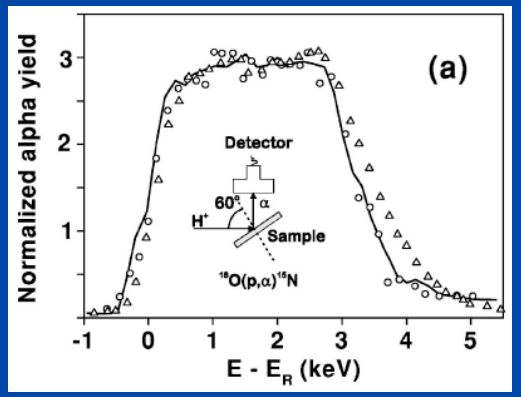

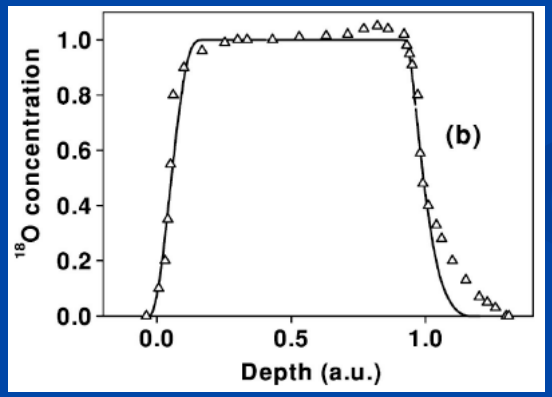

Normalized excitation curves of the $^{18}O(p,\alpha)^{15}N$ nuclear reaction around the resonance at 151 keV before and after thermal annealings and the used experimental geometry.(b) Normalized ^{18}O concentration vs. normalized depth for the as deposited and $^{18}O_2$-annealed samples.

Solid lines represent the as-deposited sample, empty circles and triangles correspond to vacuum and ^{18}O-annealed samples, respectively.

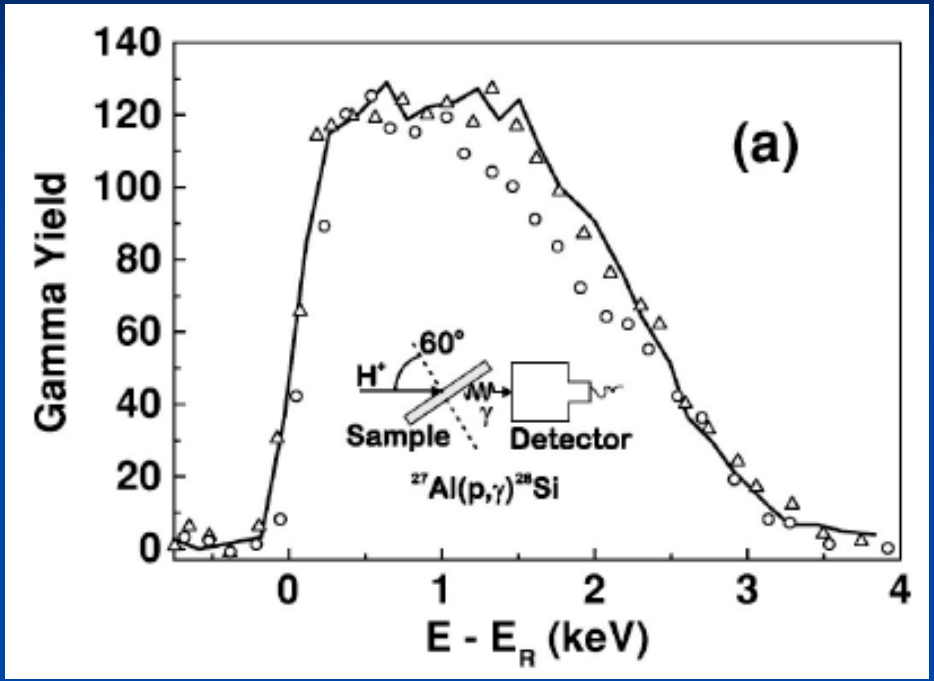

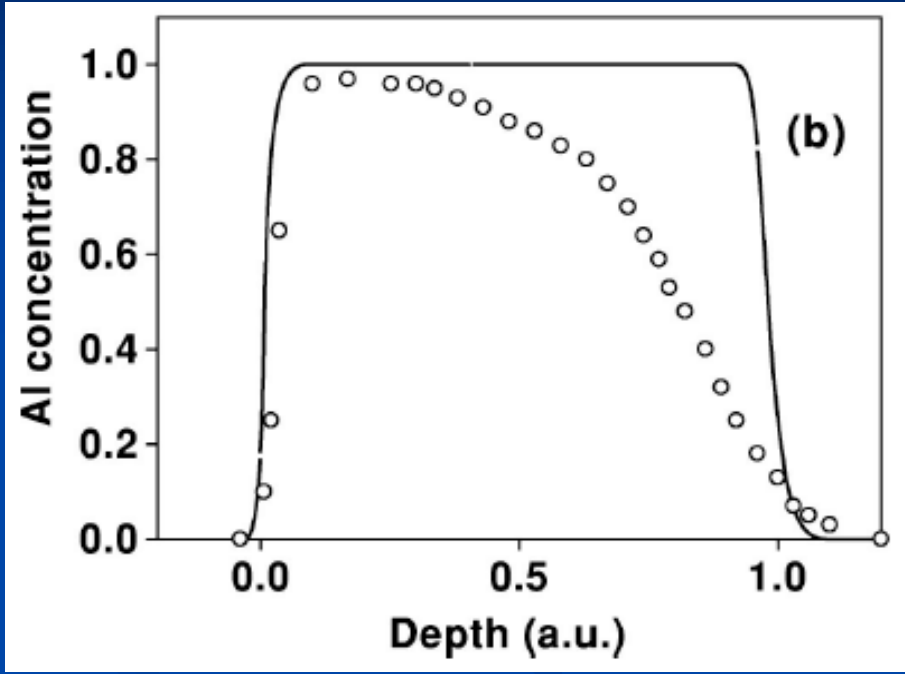

(a) Excitation curves of the $^{27}Al(p,\gamma)^{28}Si$ nuclear reaction around the resonance at 404.9 keV before and after thermal annealings and the used experimental geometry.

(b) Normalized ^{27}Al concentration vs. normalized depth for the as-deposited and vacuum-annealed samples.

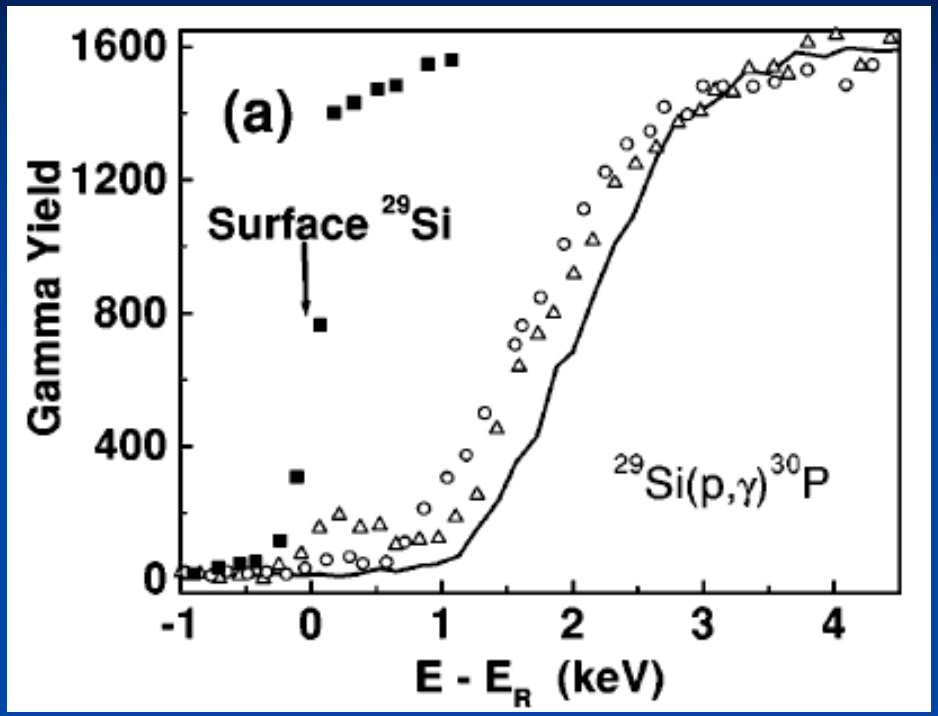

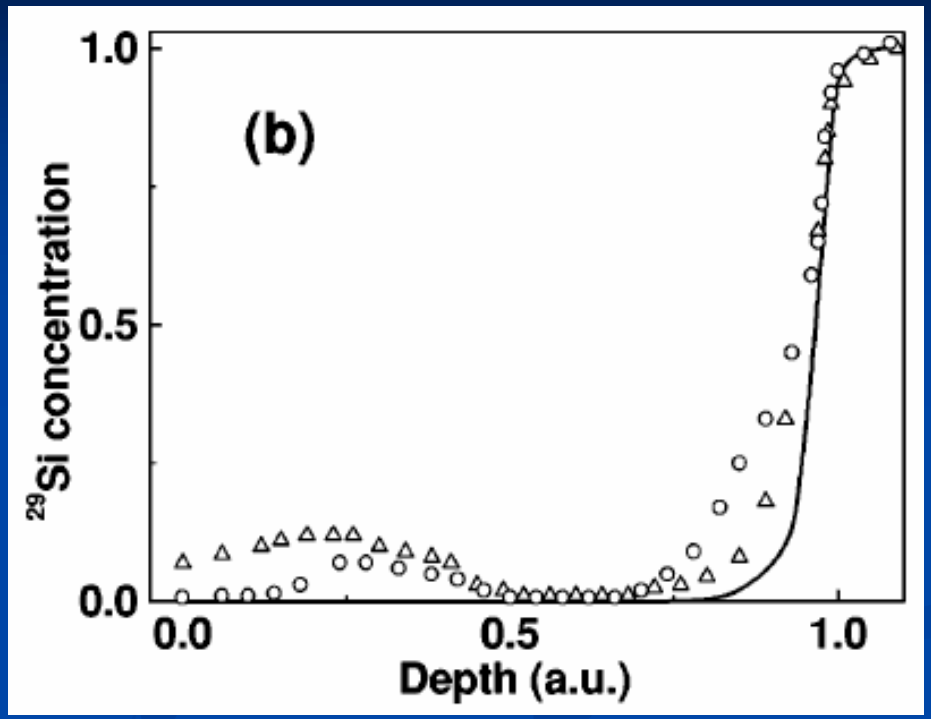

(a) Excitation curves of the ^{29}Si(p,γ)30P nuclear reaction around the resonance at 414 keV before and after thermal annealings.

(b) Normalized ^{29}Si concentration vs. normalized depth for the as-deposited, $^{18}O_2$- and vacuum-annealed samples.

Summary

- Isotope specific – unique tool for studying transport processes
- Absolute concentration by well-known reference samples (no need of exact knowledge of cross section)
- Narrow resonances: almost atomic depth resolution at the surface